

AERODYNAMIC CHARACTERISTICS OF A WEDGE AND CONE  
AT HYPERSONIC MACH NUMBERS

Thesis by  
Lt. Lee R. Scherer, Jr., U.S.N

In Partial Fulfillment of the Requirements  
For the Degree of  
Aeronautical Engineer

California Institute of Technology  
Pasadena, California

1950

## ACKNOWLEDGEMENTS

The author wishes to express his sincere appreciation to Dr. Henry T. Nagamatsu for his formulation of the problem and for his interest and guidance throughout the investigation.

Appreciation is also expressed to Mrs. Katherine McColgan, Aeronautics Librarian, whose patience and aid in ferreting out obscure references assisted materially in obtaining the necessary literature for this investigation, and to Miss Shirley Woodbury for her assistance in preparation of the manuscript.

The author is also indebted to his associate in the problem Lt. Richard D. DeLauer, USN.

## ABSTRACT

Up to the present time, the reliability of the determination of aerodynamic characteristics at hypersonic Mach numbers by theoretical calculations has been unknown due to the lack of experimental data. This report is the calculations of these characteristics by four different theories of a wedge and a cone over a range of Mach numbers from 2 to 12.

Correlation of these results with wind tunnel tests was not possible due to scheduling difficulties of the hypersonic wind tunnel; therefore, this report is designed to serve as the basis for comparison of future hypersonic experiments.

From correlation of the various theories it is found that the closest agreement to the exact theory at hypersonic speeds is given by the hypersonic similarity theory. Above Mach numbers of about 3, the first and second order theories deviate considerably from the exact theory.

## TABLE OF CONTENTS

<u>Part</u>	<u>Title</u>	<u>Page</u>
	Acknowledgments	i
	Abstract	ii
	Table of Contents	iii
	List of Figures	iv
	List of Tables	vi
	Symbols and Notation	viii
I.	Introduction	1
II.	Calculations by the Various Theories	3
	A. Oblique Shock Wave Theory for Wedge	3
	B. Exact Theory for Cone	4
	C. First Order Theory - Wedge	5
	D. First Order Theory - Cone	8
	E. Second Order Theory - Wedge	10
	F. Second Order Theory - Cone	10
	G. Hypersonic Similarity	13
III.	Conclusions	16
	References	18
	Tables	19
	Figures	41

## LIST OF FIGURES

<u>Figure No.</u>	<u>Title</u>	<u>Page</u>
1	Sketch of Wedge Model	41
2	Sketch of Cone Model	42
3	Photograph of Wedge Model	43
4	Photograph of Cone Model	43
5	Oblique Shock Theory - Wedge - $0^\circ$ Angle of Attack, $C_p$ vs M	44
6	Oblique Shock Theory - Wedge - $2^\circ$ Angle of Attack, $C_p$ vs M	45
7	Oblique Shock Theory - Wedge - $4^\circ$ Angle of Attack, $C_p$ vs M	46
8	Exact Theory - Cone, $C_p$ vs M	47
9	First Order Theory - Wedge - $0^\circ$ Angle of Attack, $C_p$ vs M	48
10	First Order Theory - Wedge - $2^\circ$ Angle of Attack, $C_p$ vs M	49
11	First Order Theory - Wedge - $4^\circ$ Angle of Attack, $C_p$ vs M	50
12	First Order Theory - Cone, $C_p$ vs M	51
13	Second Order Theory - Wedge - $0^\circ$ Angle of Attack, $C_p$ vs M	52

## LIST OF FIGURES (continued)

<u>Figure No.</u>	<u>Title</u>	<u>Page</u>
14	Second Order Theory - Wedge - $2^\circ$ Angle of Attack, $C_p$ vs M	53
15	Second Order Theory - Wedge - $4^\circ$ Angle of Attack, $C_p$ vs M	54
16	Second Order Theory - Cone, $C_p$ vs M	55
17	Hypersonic Similarity Parameters	56
18	Hypersonic Similarity - Wedge - $0^\circ$ Angle of Attack, $C_p$ vs M	57
19	Hypersonic Similarity - Wedge - $2^\circ$ Angle of Attack, $C_p$ vs M	58
20	Hypersonic Similarity - Wedge - $4^\circ$ Angle of Attack, $C_p$ vs M	59
21	Hypersonic Similarity - Cone, $C_p$ vs M	60
22	Various Theories - $20^\circ$ Wedge and Cone - $0^\circ$ Angle of Attack, $C_p$ vs M	61
23	Various Theories - $20^\circ$ Wedge - $2^\circ$ and $4^\circ$ Angles of Attack, $C_L$ vs M	62

## LIST OF TABLES

<u>Table No.</u>	<u>Title</u>	<u>Page</u>
I	$C_p$ , Oblique Shock Theory - Wedge - $0^\circ$ Angle of Attack	19
II	$C_p$ , Oblique Shock Theory - Wedge - $2^\circ$ Angle of Attack	20
III	$C_p$ , Oblique Shock Theory - Wedge - $4^\circ$ Angle of Attack	21
IV	$C_p$ , Exact Theory - Cone	22
V	$C_p$ , First Order Theory - Wedge - $0^\circ$ Angle of Attack	23
VI	$C_p$ , First Order Theory - Wedge - $2^\circ$ Angle of Attack	24
VII	$C_p$ , First Order Theory - Wedge - $4^\circ$ Angle of Attack	25
VIII	$C_p$ , First Order Theory - Cone	26
IX	$C_p$ , Second Order Theory - Wedge - $0^\circ$ Angle of Attack	27
X	$C_p$ , Second Order Theory - Wedge - $2^\circ$ Angle of Attack	28
XI	$C_p$ , Second Order Theory - Wedge - $4^\circ$ Angle of Attack	29

## LIST OF TABLES (continued)

<u>Table No.</u>	<u>Title</u>	<u>Page</u>
XII	$C_p$ , Second Order Theory - Cone	30
XIII	Hypersonic Similarity Parameters	31
XIV	$C_p$ , Hypersonic Similarity - Wedge - $0^\circ$ Angle of Attack	32
XV	$C_p$ , Hypersonic Similarity - Wedge - $2^\circ$ Angle of Attack	33
XVI	$C_p$ , Hypersonic Similarity - Wedge - $4^\circ$ Angle of Attack	36
XVII	$C_p$ , Hypersonic Similarity - Cone	39
XVIII	$C_L$ , Various Theories - $20^\circ$ Wedge	40



## SYMBOLS AND NOTATION

The following are the symbols and notation with their definitions used in this investigation.

$P_i$	static pressure of the flow. The subscripts denote flow field
	1 - free stream
	2 - flow behind shock or on body
	o - stagnation conditions
	s - flow on surface of body
$C_p$	pressure coefficient = $\Delta P/q$
$q$	free stream dynamic pressure = $\frac{1}{2} \rho U^2 = \frac{\delta P}{2} M^2$
$u_1$	free stream velocity
$a_i$	speed of sound $a_i = \sqrt{\frac{\delta P_i}{\rho_i}}$ . Subscript indicates some conditions as pressure p
$\rho_i$	fluid density. Subscripts same as for p
$M_i$	Mach number = $\frac{u_i}{a_i}$ . Subscripts same as p
$\beta$	inclination of shock wave, or the quantity $\sqrt{M_1^2 - 1}$
$\delta$	ratio of specific heats = 1.4 for air
$r, \theta$	cylindrical or spherical coordinates
$x_i$	Cartesian coordinates. Subscripts denote orthogonal directions of axis
$u, v$	velocity components

## SYMBOLS AND NOTATION (continued)

$u_i, v_k$	indicate $\frac{\partial u}{\partial l}$ , $\frac{\partial v}{\partial k}$ where i, k are coordinates of system being used
$\Theta$	semi-apex angle of cone or wedge, and flow deflection in one particular case
$\Phi$	potential notation
$\alpha$	angle of attack
$\xi, \eta, \tau$	non-dimensional coordinates, or variables of integration
$\delta$	body thickness, or total apex angle
$b$	body length
$k$	thickness ratio parameter ( $\delta/b$ )M

## I. INTRODUCTION

The purpose of this investigation was to calculate the aerodynamic characteristics of a wedge and a cone at hypersonic Mach numbers by utilizing the existing theories, and to correlate these results with actual test data.

The possibility of extending existing supersonic flow theories to hypersonic speeds has been investigated only theoretically up to this time, due to the lack of experimental data at hypersonic Mach numbers. Now the existence of a hypersonic wind tunnel makes such test data available, and this investigation is the first step in the correlation of such data with the various theories. Since there are so many ramifications to the problem, boundary layer, tunnel boundary interference, deviations from a perfect gas, etc., this is but one small phase of the vast over-all problem, and it is hoped that it will serve as a basis for future experimental work.

The principal aerodynamic characteristic obtained was the surface pressure on various angles for wedges and cones at Mach numbers ranging from 2 to 12. The four existing theories used in the determination of the theoretical pressure distribution were:

1. Oblique Shock Theory for Wedge; Exact Theory for Cone
2. First Order Theory - Linearized
3. Second Order Theory

#### 4. Hypersonic Similarity.

A brief discussion of the above theories is given in Part II.

For the theoretical calculations, the configurations used were:

1. Wedge with apex angles of  $5^\circ$ ,  $10^\circ$ ,  $20^\circ$ ,  $30^\circ$ ,  $40^\circ$ ,  $50^\circ$  and  $60^\circ$  at angles of attack of  $0^\circ$ ,  $2^\circ$ , and  $4^\circ$ .
2. Cone with apex angles of  $5^\circ$ ,  $10^\circ$ ,  $20^\circ$ ,  $30^\circ$ ,  $40^\circ$ ,  $50^\circ$  and  $60^\circ$  at angle of attack of  $0^\circ$ .

Due to lack of time, actual correlation with test data was not possible in this report. Models of a  $20^\circ$  wedge and cone were constructed, and their details are included herewith.

It is planned that this report should serve as the first phase, the basic groundwork, for the future experimental investigations of hypersonic flow.

## II. CALCULATIONS BY THE VARIOUS THEORIES

### A. Oblique Shock Wave Theory for Wedge

The pressure coefficient ( $C_p$ ) is defined as the ratio of the change in pressure ( $\Delta P$ ) to the dynamic pressure ( $q$ ).

$$C_p = \frac{(P_2 - P_1)}{q}$$

but

$$q = \frac{1}{2} \rho U_1^2 = \frac{\gamma P}{2} M_1^2$$

since

$$M_1 = \frac{U_1}{a_1} \quad \text{and} \quad a_1 = \sqrt{\frac{\gamma P_1}{\rho}}$$

Therefore,

$$C_p = \frac{\Delta P}{q} = \frac{2}{\gamma M_1^2} \frac{P_2 - P_1}{P_1}$$

The normal shock relation for  $(p_2 - p_1)/p_1$  is  $\frac{2\gamma}{\gamma+1} (M_1^2 - 1)$ .

To obtain the correct oblique shock relation, it is only necessary to replace  $M_1$  by  $M_1 \sin \beta$ , (Ref. 1). Thus,

$$\begin{aligned} \frac{P_2 - P_1}{P_1} &= \frac{2\gamma}{\gamma+1} (M_1^2 \sin^2 \beta - 1) \\ C_p &= \frac{4}{M_1^2 (\gamma+1)} (M_1^2 \sin^2 \beta - 1) \end{aligned}$$

Where the relation between the wave angle  $\beta$  and the flow deflection is

$$\frac{1}{M_1^2} = \sin^2 \beta - \frac{\gamma+1}{2} \frac{\sin \beta \sin \theta}{\cos(\beta-\theta)}$$

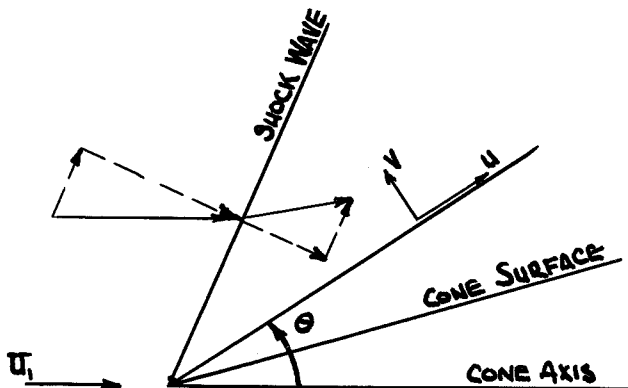
Utilizing this formula Tables I to III were computed and plotted in Figs. 5 to 7.

### B. Exact Theory for Cone

The problem of supersonic flows around cones at zero angle of attack is one of the two types of high speed flows in three-dimensions that can be discussed mathematically without objectionable simplification.

The fundamental equation of conical flow as derived by Sebert in Ref. 2 and in a similar manner by Kopal, (Ref. 3), is

$$\frac{d^2 u}{d\theta^2} + u = \frac{a^2(u + v \cot \theta)}{v^2 - a^2}$$



The solutions to this equation cannot be obtained analytically, so in order to determine them, recourse must be had to numerical intergration. This has been carried out by Kopal and put in tabular form. He tabulates the ratio of the pressure on the cone to that immediately behind the shock wave  $p_s/p_2$ , and the ratio of the pressure immediately behind the shock wave, to that of the undisturbed air in front of the shock wave,  $p_2/p_1$ . The product of these two gives  $p_s/p_1$  so  $\frac{\Delta P}{P_1}$  can be calculated, by

$$\frac{P_s}{P_1} - 1 = \frac{P_s - P_1}{P_1}$$

and

$$C_p = \frac{2}{\gamma M_1^2} \frac{P_s - P_1}{P_1}$$

Following this procedure the data of Table IV were calculated and plotted in Fig. 8.

### C. First Order Theory - Wedge

By assuming irrotational flow and linearizing the equations of motion, a perturbation potential may be introduced. Considering a uniform rectilinear velocity  $U$  at  $\infty$ , it is assumed that the deviations of the velocity from  $U$  are small, and squares and higher powers of these perturbation velocities are neglected. This assumption corresponds to limiting the solid boundaries to shapes whose inclination to  $U$  is always small.

The linearized equation of motion becomes, (Ref. 4)

$$\left(1 - \frac{U^2}{a_0^2}\right) \frac{\partial u_1'}{\partial x_1} + \frac{\partial u_2'}{\partial x_2} + \frac{\partial u_3'}{\partial x_3} = 0$$

where

(away from body)	(neighborhood of body)
$u_1 = U = \text{constant}$	$u_1 = U = u_1'$
$u_2 = 0$	$u_2 = u_2'$
$u_3 = 0$	$u_3 = u_3'$

In terms of the potential function

$$\Phi = Ux_1 + \phi(x_i)$$

$$u_i = \frac{\partial \phi}{\partial x_i} \ll U$$

where  $\phi(x_i)$  is the perturbation potential. The linearized perturbation potential equation becomes

$$(1 - M_\infty^2) \frac{\partial^2 \phi}{\partial x_1^2} + \frac{\partial^2 \phi}{\partial x_2^2} + \frac{\partial^2 \phi}{\partial x_3^2} = 0$$

The same approximations are used for determining the pressure coefficient. The exact relationship for  $p/p_0$  is

$$\frac{p}{p_0} = \left[ \frac{1 - \frac{\gamma-1}{2} M_\infty^2}{1 + \frac{\gamma-1}{2} M^2} \right]^{\frac{\gamma}{\gamma-1}}$$



Linearized, this is

$$\frac{p_2}{p_1} = \left[ \frac{1}{1 + \frac{\gamma-1}{2} M_1^2 \frac{2u'}{U}} \right]$$

Expanding, we have

$$\frac{p_2}{p_1} = 1 - \frac{\gamma}{2} M_1^2 \frac{2u'}{U} + \dots$$

Since

$$\frac{\gamma}{2} M_1^2 p_1 = \frac{1}{2} \rho_1 U_1^2$$

thus,

$$C_p = -2 \frac{u'}{U}$$

By solving the perturbation equation together with the boundary conditions that the normal derivative of  $\phi$  vanishes at all solid boundaries, the pressure coefficient equation becomes

$$C_p = \frac{2}{\sqrt{M_1^2 - 1}} \left[ \frac{dx_2}{dx_1} \right]_{\text{boundary}}$$

For the wedge  $\frac{dx_2}{dx_1}$  boundary is merely the tangent of the semi-apex angle  $\Theta$ , or

$$C_p = \frac{2}{\sqrt{M_1^2 - 1}} \text{TAN } \Theta$$

For the wedge at angles of attack, this same equation holds by merely subtracting or adding  $\alpha$  to  $\theta$  for the upper or lower surfaces.

These calculations are given in Tables V, VI, and VIII and are plotted in Figs. 9, 10, and 11.

#### D. First Order Theory - Cone

Following von Kármán, (Ref. 5), the linearized potential equation in cylindrical coordinates with axial symmetry is

$$\frac{\partial^2 \Phi}{\partial r^2} + \frac{1}{r^2} \frac{\partial \Phi}{\partial r} + \left(1 - \frac{U^2}{a^2}\right) \frac{\partial^2 \Phi}{\partial x^2} = 0$$

Assuming that the effects of infinitesimals can be superimposed, the potential of the additional velocities has the form

$$\Phi(x, r) = \int_0^{x-\beta r} \frac{f(\xi) d\xi}{\sqrt{(x-\xi)^2 - \beta^2 r^2}}$$

where

$$\beta = \sqrt{M^2 - 1}$$

Placing the origin at the vertex of the body, this integral can be transformed by letting

$$\frac{x-\xi}{\beta r} = \cosh u$$

The potential expression becomes

$$\Phi = \int_{\cosh \frac{x}{\beta r}}^0 f(x - \beta r) \cosh u \, du$$

and the velocity components are

$$\frac{\partial \Phi}{\partial x} \quad \text{and} \quad \frac{\partial \Phi}{\partial r}$$

By solving the above equation von Kármán obtained for the over pressure acting on the cone

$$\Delta p = \rho U^2 \theta^2 \frac{\cosh^{-1} \left( \frac{1}{\theta \beta} \right)}{\sqrt{1 - \frac{\theta^2}{\beta^2} + \theta \cosh^{-1} \frac{1}{\theta \beta}}}$$

which is approximately

$$\Delta p = \rho U^2 \theta^2 \ln \left( \frac{2}{\theta \beta} \right)$$

Thus

$$C_p = 2\theta^2 \ln \frac{2}{\theta \sqrt{M^2 - 1}}$$

The calculated results of this equation is given in Table VIII and plotted in Fig. 12.

### E. Second Order Theory - Wedge

The next step to the linearization procedure used in the previous section in an iteration procedure corresponding to the general technique of solution by successive approximations based on the theory of perturbations, is the second approximation which may be made by several different approaches. By introducing a parameter  $\tau$  proportional to the thickness ratio of the body under consideration, the potential function may be expanded in a power series in  $\tau$ . This has been carried out by Busemann, (Ref. 6), for a two-dimensional supersonic flow.

The Busemann second approximation for the pressure coefficient is

$$C_p = \pm \frac{2}{\sqrt{M^2-1}} \theta + \frac{\gamma M^4 + (M^2-2)^2 \theta^2}{2(M^2-1)^2}$$

$\theta$  is the angle of flow deflection, the semi-apex angle at zero angle of attack. The computations based on this equation are given in Tables IX, X, and XI and are plotted in Figs. 13, 14, and 15.

### F. Second Order Theory - Cone

For axially-symmetric flow, the discovery of a particular solution of the iteration equation has reduced the problem of determining a second-order approximation to one of first-order.

Following Van Dyke, (Ref. 7), the iteration equation for a cone is

$$(1-t^2)\bar{\Phi}_{tt} + \frac{\bar{\Phi}_t}{t} = M^2 \left[ 2(N-1)t^2\bar{\Phi}_{tt} (\bar{\Phi} - t\bar{\Phi}_t) - 2t\bar{\Phi}_{tt} + \bar{\Phi}_t + \beta^2\bar{\Phi}_{tt}\bar{\Phi}_t^2 \right]$$

where  $(x, t)$  are the conical non-orthogonal coordinates and

$$t = \frac{\beta r}{x} \quad \beta = \sqrt{M^2 - 1} \quad N = \frac{(\gamma + 1)M^2}{2\beta^2}$$

$$\bar{\Phi}(x, t, \theta) = x\bar{\Phi}(t, \theta)$$

$$\bar{\Phi}_r = \beta\bar{\Phi}_t$$

$$\bar{\Phi}_x = \bar{\Phi} - t\bar{\Phi}_t$$

$$\bar{\Phi}_{rr} = \frac{\beta^2}{x}\bar{\Phi}_{tt}$$

$$\bar{\Phi}_{xx} = \frac{t^2}{x}\bar{\Phi}_{tt}$$

$$\bar{\Phi}_{xr} = -\frac{\beta t}{x}\bar{\Phi}_{tt}$$

$\bar{\Phi}$  is first order perturbation potential  
 $\bar{\Phi}^{(2)} = \bar{\Phi} + \Phi$  is second order perturbation potential

The boundary conditions for the second order solution are

$$\frac{\bar{\Phi}_r}{1 + \bar{\Phi}_r} = \text{slope}$$

$$\beta\bar{\Phi}_t(\beta\epsilon) = \epsilon [\varphi(\beta\epsilon) - \beta\epsilon\bar{\Phi}_t(\beta\epsilon)]$$

$$\bar{\Phi}(\infty) = \bar{\Phi}_t(\infty) = 0$$

The cone has a semi-apex angle  $\tan^{-1} \epsilon$ . Using the integrating factor

$\frac{t}{\sqrt{1-t^2}}$ , the equation can be integrated to give the result

$$\bar{\Phi} = -A (\text{sech}^{-1} t - \sqrt{1-t^2})$$

where  $A = \frac{\epsilon^2}{\sqrt{1-\beta^2\epsilon^2} + \epsilon^2 \text{sech}^{-1}(\beta\epsilon)}$

Substituting the first order solution into the iteration equation and using the same integrating factor again, Van Dyke obtains for the complete conical second-order perturbation potential

$$\begin{aligned} \bar{\Phi}^{(2)}(t) = & -A (\text{sech}^{-1} t - \sqrt{1-t^2}) + 4M^2 [B (\text{sech}^{-1} t - \sqrt{1-t^2}) \\ & + (\text{sech}^{-1} t)^2 - (N+1)\sqrt{1-t^2} \text{sech}^{-1} t - \frac{\beta^2 A}{4} \frac{\sqrt{1-t^2}}{t^2}] \end{aligned}$$

The streamwise and radial velocity perturbations are

$$\begin{aligned} \frac{u}{U} = & -A \text{sech}^{-1} t + A^2 M^2 [B \text{sech}^{-1} t + (\text{sech}^{-1} t)^2 - (N-1) \frac{\text{sech}^{-1} t}{\sqrt{1-t^2}} \\ & - (N+1) - \frac{3}{4} \beta^2 A \frac{\sqrt{1-t^2}}{t^2}] \\ \frac{1}{\beta} \frac{v}{U} = & A \frac{\sqrt{1-t^2}}{t} + A^2 M^2 [-B \frac{\sqrt{1-t^2}}{t} - 2 \frac{\sqrt{1-t^2} \text{sech}^{-1} t}{t} + (N+1) \frac{1}{t} \\ & + (N-1) \frac{t \text{sech}^{-1} t}{\sqrt{1-t^2}} + \frac{1}{2} \beta^2 A \frac{\sqrt{1-t^2}}{t^3}] \end{aligned}$$

B must be adjusted to satisfy the tangency condition. It is easiest to do this numerically in actual computation. From these results, the pressure coefficient can be calculated as

$$C_p = \frac{2}{\gamma M^2} \left\{ \left[ 1 - \frac{\gamma-1}{2} M^2 \left( 1 - \frac{q^2}{U^2} \right) \right]^{\frac{\gamma}{\gamma-1}} - 1 \right\}$$

These calculated values are given in Table XII and plotted in Fig. 16.

#### G. Hypersonic Similarity

Tsien, (Ref. 8), has developed the similarity laws for hypersonic flows. An affined transformation which expands the flow field laterally reduces the equations of the flows to a single non-dimensional equation. If a series of bodies having the same thickness distribution but different thickness ratio,  $\delta/b$ , are put into flows of different Mach numbers  $M_1$  such that the products of  $M_1$  and  $\delta/b$  remains constant and equal to  $K$ , then the flow patterns are similar in that they are governed by the same transformed velocity potential.

For flow over cones, Hayes, (Ref. 9), interpretation is the propagation of cylindrical waves from a uniformly expanding circular cylinder. To solve the associated wave problem, it is observed that the radial velocity  $v$ , the pressure  $p$ , and the density  $\rho$  are functions of  $S = y/t$  only. That is,

$$\left( \frac{\partial}{\partial t} + \frac{y}{t} \frac{\partial}{\partial y} \right) (v, p, \rho) = 0$$

The equations of equilibrium and continuity become

$$(v-s) \frac{dv}{ds} = -\frac{1}{\rho} \frac{dp}{ds}$$

$$\left(\frac{v-s}{\rho}\right) \frac{d\rho}{ds} + \frac{dv}{ds} + \frac{v}{s} = 0$$

Introducing the following changes of variable

$$\mu = \frac{v}{s} \quad \beta = \frac{a^2}{s^2} \quad \sigma = \ln s$$

where  $\mu$  is the new independent variable and "a" denotes the local velocity of sound, the equations above are transformed into

$$\frac{d\beta}{d\mu} = \frac{2\beta}{\mu} \beta + \frac{[\frac{1}{2}(\gamma+1)\mu - 1](1-\mu)}{2\beta - (1-\mu)^2}$$

$$\frac{d\sigma}{d\mu} = -\frac{1}{\mu} \frac{\beta - (1-\mu)^2}{2\beta - (1-\mu)^2}$$

Shen, (Ref. 10), solves these basic equations by expanding the solution into a series near the initial point and using a standard numerical integration thereafter. From these results, the pressure ratio at the cone surface  $p_s/p_1$  can be obtained. Calling the cone half-angle  $\Theta$ , we have

$$K = M_1 \Theta$$



Now

$$C_p = \frac{2}{\gamma M_1^2} \left( \frac{p_2}{p_1} - 1 \right)$$

$$\frac{C_p}{\Theta^2} = \frac{2}{\gamma K^2} \left( \frac{p_2}{p_1} - 1 \right)$$

Keeping the similarity parameter  $K$  constant will give the same flow pattern. Thus, a single curve of  $C_p/\Theta^2$  vs  $K$  suffices for various slender cones in hypersonic flows.

Using Shen's tabulated results of  $K$  vs  $C_p/\Theta^2$  it is a simple matter to expand to values of  $M$  and  $C_p$  for various  $\Theta_s$ . These results are given in Table XVI and are plotted in Fig. 21.

For hypersonic flow over wedges Shen's procedure gives

$$\frac{C_p}{\Theta^2} = \frac{\gamma+1}{2} + 2\sqrt{\left(\frac{\gamma+1}{4}\right)^2 + \frac{1}{K^2}}$$

Utilizing this equation, Table XIII of various values of  $C_p/\Theta^2$  and  $K$  is obtained. These results are expanded as before for values of  $M$  and  $C_p$  for various  $\Theta_s$ . These data are given in Tables XIV, XV, and XVI and are plotted in Figs. 18, 19, and 20.

## CONCLUSIONS

The conclusions of principal interest in the basic problem will result from the correlation of the experimental data with that calculated from the various existing theories. Since in this report such correlation is not as yet possible recourse must be had to a comparison of the various theories themselves.

For this purpose Fig. 22 has been plotted. This figure is a cross-plot of Mach number versus surface pressure coefficient as calculated by the various theories for the model wedge and cone, i.e., for a  $20^\circ$  total apex angle. From a study of this curve, the following conclusions may be drawn:

1. The first order theory gives values which are lower than those of the exact or oblique shock theory throughout the entire Mach number range. The amount of deviation increases with the Mach number.
2. The second order theory gives close agreement with the exact theory at low Mach numbers (below  $M = 4$ ), and is much closer than the first order theory throughout the entire range.
3. The range over which first and second order theories may be used is limited by the form of the equations. This range is determined by the apex angle. For the  $20^\circ$  cone, imaginary results are obtained above Mach number of 11.0 by the first order theory and above Mach number of 5.7 by the second order theory.

4. At the higher Mach numbers (above 6) excellent agreement is obtained between the hypersonic similarity and exact solutions.

The lift coefficients for the  $20^\circ$  wedge at  $2^\circ$  and  $4^\circ$  angles of attack were calculated and plotted in Fig. 23. The same pattern of deviations between the exact and other theories is found as with the pressure coefficients.

## REFERENCES

1. Millikan, C. B., "Hydrodynamics of Compressible Fluids", AE 261 Lecture Notes, California Institute of Technology, 1949-1950.
2. Sebert, Harold W., "High Speed Aerodynamics", Prentice-Hall, Inc., pp. 180-197, New York, 1948.
3. Kopal, Z., "Tables of Supersonic Flow Around Cones", Tech. Report No. 1, Massachusetts Institute of Technology, Department of Electrical Engineering, Center of Analysis, 1947.
4. Liepmann, H. W. and Puckett, A. E., "Aerodynamics of a Compressible Fluid", GALCIT Aeronautical Series, John Wiley and Sons, Inc., pp. 121-124, New York, 1947.
5. Von Kármán, Th., "The Problem of Resistance in Compressible Fluid", Proc. of the 5th Volta Congress, pp. 275-277, Rome, 1936.
6. Busemann, A., "The Achsensymmetrische Kegelge Ukershallstromung", Luftfahrtforschung, pp. 157-144, 1942.
7. Van Dyke, M. D., "A Study of Second-Order Supersonic Flow", Ph. D. Thesis, California Institute of Technology, 1949.
8. Tsien, H. S., "Similarity Laws of Hypersonic Flows", Jour. of Math. and Phys., Vol. 25, pp. 56-66, 1948.
9. Hayes, W. D., "On Hypersonic Similitude", Quart. of Appl. Math., Vol. 5, p. 105, 1947.
10. Shen, S. F., "Hypersonic Flow Over a Slender Cone", Jour. of Math. and Phys., Vol. 27, pp. 56-66, 1948.

TABLE I

Wedge

Oblique Shock Theory

 $\alpha^\circ$  Angle of Attack $C_p$  $\delta$ 

M	$5^\circ$	$10^\circ$	$20^\circ$	$30^\circ$	$40^\circ$	$50^\circ$	$60^\circ$
2.0	.0716	.110	.2565	.433	.665		
4.0	.0241	.0558	.1531	.2425	.379	.581	.738
6.0	.0177	.046	.106	.203	.329	.484	.666
8.0	.0148	.0325	.0939	.187	.3095	.463	.641
10.0	.0116	.0294	.0871	.1765	.302	.4515	.634
12.0		.026	.0835	.172	.295	.443	.625

TABLE II

## Wedge

## Oblique Shock Theory

2° Angle of Attack

M		$\delta$						
		5°	10°	20°	30°	40°	50°	60°
2.0	C <sub>p</sub> upper	.0133	.070	.192	.352	.556	.94	
	lower	.104	.168	.320	.51	.800		
4.0	C <sub>p</sub> upper	.0045	.038	.100	.194	.324	.476	.652
	lower	.050	.086	.170	.298	.444	.612	.826
6.0	C <sub>p</sub> upper	.0028	.026	.078	.162	.276	.420	.590
	lower	.040	.068	.142	.250	.384	.552	.742
8.0	C <sub>p</sub> upper	.0022	.018	.066	.146	.260	.396	.566
	lower	.030	.052	.128	.236	.368	.530	.720
10.0	C <sub>p</sub> upper	.0015	.012	.060	.140	.256	.390	.560
	lower	.026	.050	.120	.230	.360	.520	.710
12.0	C <sub>p</sub> upper	.0011	.012	.060	.140	.256	.390	.560
	lower	.026	.050	.116	.230	.360	.520	.710

TABLE III

Wedge

Oblique Shock Theory

4° Angle of Attack

M		$\delta$						
		5°	10°	20°	30°	40°	50°	60°
2.0	C <sub>p</sub> upper		.025	.140	.290	.470	.720	
	lower	.154	.224	.390	.608			
4.0	C <sub>p</sub> upper		.0109	.072	.150	.270	.414	.578
	lower	.080	.116	.220	.354	.506	.692	.924
6.0	C <sub>p</sub> upper		.0069	.052	.124	.226	.360	.518
	lower	.060	.092	.184	.304	.450	.590	.830
8.0	C <sub>p</sub> upper		.0042	.044	.110	.212	.340	.494
	lower	.050	.080	.170	.288	.428	.566	.800
10.0	C <sub>p</sub> upper		.0040	.040	.104	.206	.334	.486
	lower	.044	.076	.160	.280	.420	.560	.790
12.0	C <sub>p</sub> upper		.0037	.040	.100	.206	.330	.480
	lower	.044	.076	.160	.280	.420	.556	.786

TABLE IV

Cone  
Exact Theory (Kopal)  
0° Angle of Attack  
 $C_p$

$\delta$

M	10°	20°	30°	40°	50°	60°
2.0	.0348	.1046	.2026	.3240	.473	.641
4.0	.0250	.0801	.1600	.2670	.382	.551
6.0	.0217	.0720	.1500	.2565	.375	.534
8.0	.0188	.0676	.1465	.2530	.365	.524
10.0	.0186	.0669	.1440	.2520	.363	.519
12.0	.0178	.0658	.1415	.2520	.363	.519



TABLE V

Wedge

First Order Theory

 $0^\circ$  Angle of Attack $C_p$ 

M	$\delta$						
	$5^\circ$	$10^\circ$	$20^\circ$	$30^\circ$	$40^\circ$	$50^\circ$	$60^\circ$
2.0	.0503	.1006	.2035	.3090	.4200	.5280	.6650
4.0	.0225	.0449	.0909	.1380	.1880	.2410	.2975
6.0	.0148	.0295	.0596	.0906	.1232	.1580	.1953
8.0	.0110	.0219	.0443	.0673	.0914	.1172	.1450
10.0	.0088	.0175	.0355	.0539	.0732	.0939	.1160
12.0	.0073	.0146	.0295	.0448	.0608	.0780	.0965

TABLE VI

Wedge

First Order Theory

2° Angle of Attack

M		$\delta$						
		5°	10°	20°	30°	40°	50°	60°
2.0	C <sub>p</sub> upper	0	.0604	.1625	.2665	.3755	.4900	.6130
	lower	.0905	.1420	.2455	.3530	.4670	.5880	.7220
4.0	C <sub>p</sub> upper	0	.0269	.0725	.1190	.1678	.2190	.2740
	lower	.0404	.0633	.1096	.1577	.2085	.2625	.3220
6.0	C <sub>p</sub> upper	0	.0177	.0476	.0781	.1100	.1435	.1800
	lower	.0265	.0416	.0718	.1035	.1368	.1723	.2115
8.0	C <sub>p</sub> upper	0	.0131	.0354	.0580	.0876	.1066	.1335
	lower	.0197	.0309	.0533	.0768	.1015	.1280	.1570
10.0	C <sub>p</sub> upper	0	.0105	.0283	.0464	.0654	.0854	.1070
	lower	.0158	.0247	.0426	.0615	.0813	.1025	.1258
12.0	C <sub>p</sub> upper	0	.0087	.0235	.0386	.0544	.0709	.0888
	lower	.0131	.0205	.0355	.0511	.0675	.0852	.1045

TABLE VII

Wedge

First Order Theory

4° Angle of Attack

M		$\delta$						
		5°	10°	20°	30°	40°	50°	60°
2.0	C <sub>p</sub> upper	-.0302	.0201	.1214	.2240	.3315	.4430	.5630
	lower	.1312	.1830	.2880	.3975	.5140	.6390	.7780
4.0	C <sub>p</sub> upper	-.0135	.0090	.0542	.1000	.1480	.1980	.2510
	lower	.0588	.0816	.1288	.1775	.2295	.2855	.3475
6.0	C <sub>p</sub> upper	-.0089	.0059	.0356	.0656	.0970	.1300	.1650
	lower	.0385	.0536	.0844	.1165	.1508	.1875	.2280
8.0	C <sub>p</sub> upper	-.0066	.0044	.0264	.0488	.0720	.0963	.1225
	lower	.0286	.0398	.0626	.0865	.1118	.1391	.1695
10.0	C <sub>p</sub> upper	-.0053	.0035	.0212	.0391	.0577	.0772	.0980
	lower	.0229	.0319	.0502	.0693	.0895	.1115	.1358
12.0	C <sub>p</sub> upper	-.0044	.0029	.0176	.0324	.0479	.0642	.0815
	lower	.0190	.0265	.0417	.0575	.0745	.0925	.1127

TABLE VIII

Cone

First Order Theory

 $0^\circ$  Angle of Attack $C_p$ 

M	$\delta$						
	$5^\circ$	$10^\circ$	$20^\circ$	$30^\circ$	$40^\circ$	$50^\circ$	$60^\circ$
2.0	.0134	.0394	.1148	.2036	.2932	.3720	.4400
4.0	.0094	.0268	.0658	.0930	.0952	.0646	
6.0	.0078	.0206	.0402	.0354			
8.0	.0066	.0162	.0220				
10.0	.0038	.0127	.0080				
12.0	.0031	.0099					

TABLE IX

Wedge

Second Order Theory

 $0^\circ$  Angle of Attack $C_p$  $\delta$ 

M	$\delta$						
	$5^\circ$	$10^\circ$	$20^\circ$	$30^\circ$	$40^\circ$	$50^\circ$	$60^\circ$
2.0	.0531	.1065	.2460	.4020	.5810	.7820	1.0000
4.0	.0253	.0519	.1276	.2190	.3300	.4590	.6070
6.0	.0170	.0371	.0960	.1721	.2651	.3775	.5087
8.0	.0133	.0300	.0808	.1481	.2346	.3488	.4625
10.0	.0111	.0257	.0720	.1359	.2168	.3262	.4352
12.0	.0096	.0229	.0660	.1257	.2045	.3108	.4165

TABLE X

Wedge

Second Order Theory

 $2^\circ$  Angle of Attack

M		$\delta$						
		$5^\circ$	$10^\circ$	$20^\circ$	$30^\circ$	$40^\circ$	$50^\circ$	$60^\circ$
2.0	$C_p$ upper	.0101	.0644	.1898	.3371	.5070	.6990	.9160
	lower	.0996	.1627	.3054	.4717	.6600	.8695	1.1040
4.0	$C_p$ upper	.0045	.0304	.0960	.1803	.2832	.4050	.5460
	lower	.0480	.0811	.1615	.2614	.3795	.5161	.6720
6.0	$C_p$ upper	.0030	.0233	.0709	.1389	.2255	.3306	.4554
	lower	.0340	.0593	.1236	.2069	.3085	.4282	.5655
8.0	$C_p$ upper	.0022	.0165	.0586	.1189	.1978	.2954	.4118
	lower	.0271	.0486	.1053	.1809	.2744	.3862	.5162
10.0	$C_p$ upper	.0018	.0138	.0515	.1075	.1820	.2746	.3863
	lower	.0232	.0424	.0946	.1657	.2547	.3622	.4875
12.0	$C_p$ upper	.0015	.0121	.0468	.0994	.1707	.2605	.3693
	lower	.0204	.0383	.0874	.1554	.2411	.3457	.4675

TABLE XI

Wedge

Second Order Theory

4° Angle of Attack

M		$\delta$						
		5°	10°	20°	30°	40°	50°	60°
2.0	C <sub>p</sub> upper	-.0292	.0205	.1369	.2752	.4357	.6220	.8265
	lower	.1497	.2113	.3685	.5446	.7400	.9600	1.2010
4.0	C <sub>p</sub> upper	-.0127	.0094	.0674	.1441	.2396	.3555	.4875
	lower	.0742	.1112	.1990	.3070	.4316	.5760	.7388
6.0	C <sub>p</sub> upper	-.0081	.0063	.0487	.1094	.1884	.2872	.4035
	lower	.0539	.0830	.1544	.2458	.3541	.4815	.6266
8.0	C <sub>p</sub> upper	-.0058	.0048	.0395	.0927	.1640	.2551	.3632
	lower	.0441	.0692	.1330	.2163	.3172	.4367	.5740
10.0	C <sub>p</sub> upper	-.0045	.0039	.0342	.0830	.1499	.2358	.3393
	lower	.0383	.0613	.1206	.1995	.2952	.4098	.5422
12.0	C <sub>p</sub> upper	-.0036	.0033	.0307	.0763	.1401	.2222	.3237
	lower	.0344	.0558	.1121	.1878	.2805	.3921	.5217

TABLE XII

Cone

Second Order Theory

$\delta = 10^\circ$		$\delta = 20^\circ$		$\delta = 30^\circ$		$\delta = 40^\circ$	
M	$C_p$	M	$C_p$	M	$C_p$	M	$C_p$
3.94	.0253	2.14	.1010	1.60	.2270	1.70	.3476
7.68	.0207	3.01	.0881	2.68	.1837	2.80	.3155
11.36	.0209	3.91	.0824	3.33	.1829		
		5.48	.0821				
		5.70	.0829				



TABLE XIII

## Hypersonic Similarity Parameters

Wedge		Cone (Ref. 8)	
K	$C_p/\theta^2$	K	$C_p/\theta^2$
.1	15.200	.66	2.95
.2	11.280	.92	2.65
.3	7.980	1.22	2.45
.4	6.360	1.59	2.31
.5	5.380	2.10	2.20
.6	4.740	2.74	2.14
.8	3.980	4.00	2.10
1.0	3.536		
1.5	2.992		
2.0	2.762		
3.0	2.762		
4.0	2.500		
5.0	2.464		
6.0	2.446		
7.0	2.432		

TABLE XIV

Wedge

Hypersonic Similarity

0° Angle of Attack

5° δ		10° δ		20° δ		30° δ		40° δ		50° δ		60° δ	
M	C <sub>p</sub>	M	C <sub>p</sub>	M	C <sub>p</sub>	M	C <sub>p</sub>	M	C <sub>p</sub>	M	C <sub>p</sub>	M	C <sub>p</sub>
2.30	.0289	2.29	.0869	1.70	.249	1.87	.388	2.20	.454	2.14	.775	1.75	1.17
4.59	.0224	3.43	.0615	2.27	.198	2.24	.341	2.75	.402	3.22	.655	2.62	1.00
6.86	.0152	4.57	.0490	2.83	.168	2.99	.287	4.12	.341	4.29	.605	3.49	.916
9.16	.0121	5.71	.0415	3.40	.148	3.74	.254	5.50	.315	6.44	.565	5.23	.857
11.45	.0102	6.86	.0365	4.54	.124	5.60	.215	8.25	.294	8.59	.548	6.99	.830
		9.15	.0306	5.67	.111	7.46	.199	11.00	.285	10.70	.540	8.72	.819
		11.40	.0272	8.50	.0934	11.40	.186					10.45	.812
												12.20	.808

TABLE XV

## Wedge

Hypersonic Similarity

2° Angle of Attack

<u>5° δ</u>				<u>10° δ</u>			
M	C <sub>Pu</sub>	M	C <sub>PL</sub>	M	C <sub>Pu</sub>	M	C <sub>PL</sub>
11.50	.00115	2.50	.0710	1.92	.041	1.63	.170
		3.80	.0530	3.85	.030	2.44	.120
		5.06	.0400	5.76	.022	3.25	.096
		6.32	.0336	7.70	.017	4.06	.081
		7.60	.0282	9.60	.014	4.89	.071
		10.20	.0250	11.50	.013	6.50	.060
		12.60	.0223			8.14	.054
						12.20	.045

TABLE XV (continued)

Wedge

Hypersonic Similarity

2° Angle of Attack

<u>20° δ</u>				<u>30° δ</u>			
M	C <sub>Pu</sub>	M	C <sub>PL</sub>	M	C <sub>Pu</sub>	M	C <sub>PL</sub>
2.13	.160	1.88	.289	2.16	.285	1.96	.445
2.84	.127	2.35	.245	2.60	.251	2.62	.374
3.55	.108	2.82	.215	3.46	.211	3.28	.332
4.26	.095	3.76	.181	4.34	.187	4.90	.281
5.78	.080	4.70	.161	6.50	.159	6.54	.259
7.10	.071	7.04	.136	8.65	.146	9.80	.242
10.60	.060	9.40	.125	10.80	.137	13.20	.235
		14.00	.117				

TABLE XV (continued)

Wedge

Hypersonic Similarity

2° Angle of Attack

<u>40° δ</u>				<u>50° δ</u>			
M	C <sub>Pu</sub>	M	C <sub>PL</sub>	M	C <sub>Pu</sub>	M	C <sub>PL</sub>
2.39	.422	1.98	.654	1.88	.720	1.96	.925
3.00	.375	2.47	.580	2.35	.640	2.94	.780
4.58	.317	3.71	.490	3.53	.540	3.92	.721
5.96	.293	4.95	.453	4.70	.500	5.89	.694
8.95	.274	7.42	.424	7.06	.466	7.85	.654
12.00	.265	9.90	.410	9.40	.453	9.80	.646
		12.30	.404	11.75	.445	11.75	.640

<u>60° δ</u>			
M	C <sub>Pu</sub>	M	C <sub>PL</sub>
1.88	1.010	2.40	1.170
2.82	.850	3.20	1.080
3.75	.786	4.80	1.010
5.73	.735	6.40	.980
7.50	.712	8.00	.964
9.40	.700	9.60	.960
11.20	.700	11.20	.952

TABLE XVI

Wedge

Hypersonic Similarity

4° Angle of Attack

<u>5° δ</u>				<u>10° δ</u>			
M	C <sub>pu</sub>	M	C <sub>PL</sub>	M	C <sub>pu</sub>	M	C <sub>PL</sub>
		2.64	.107	5.70	.0045	1.90	.197
		3.53	.083	11.40	.0035	2.54	.159
		4.40	.070			3.16	.134
		5.26	.062			3.80	.118
		7.03	.052			5.06	.099
		8.80	.046			6.34	.089
		13.10	.039			9.50	.075
						12.60	.069

TABLE XVI (continued)

## Wedge

## Hypersonic Similarity

## 4° Angle of Attack

<u>20° δ</u>				<u>30° δ</u>			
M	C <sub>Pu</sub>	M	C <sub>PL</sub>	M	C <sub>Pu</sub>	M	C <sub>PL</sub>
1.90	.123	2.01	.354	2.06	.248	2.32	.475
2.86	.088	2.41	.294	2.58	.210	2.91	.421
3.80	.070	3.21	.247	3.10	.185	4.36	.356
4.76	.059	4.01	.220	4.13	.155	5.80	.329
5.70	.052	6.01	.185	5.16	.138	8.70	.307
7.60	.044	8.02	.171	7.71	.116	11.60	.298
9.50	.039	12.00	.160	10.60	.108		
10.50	.033						

TABLE XVI (continued)

Wedge

Hypersonic Similarity

4° Angle of Attack

<u>40° δ</u>				<u>50° δ</u>			
M	C <sub>Pu</sub>	M	C <sub>PL</sub>	M	C <sub>Pu</sub>	M	C <sub>PL</sub>
2.09	.394	2.25	.705	2.08	.590	2.70	.925
2.79	.330	3.37	.595	2.60	.524	3.61	.854
3.49	.294	4.50	.550	3.90	.443	5.42	.796
5.21	.248	6.74	.514	5.20	.408	7.22	.773
6.96	.229	9.00	.498	7.80	.382	9.01	.760
10.50	.214	11.20	.490	10.40	.370	10.80	.756
				13.00	.364		

<u>60° δ</u>			
M	C <sub>Pu</sub>	M	C <sub>PL</sub>
2.05	.845	2.22	1.37
3.07	.715	2.96	1.26
4.10	.660	4.45	1.18
6.15	.616	5.92	1.14
8.20	.598	7.40	1.12
10.20	.589	8.90	1.11
12.20	.580	10.70	1.11



TABLE XVII

Cone

Hypersonic Similarity

0° Angle of Attack

10° δ		20° δ		30° δ		40° δ		50° δ		60° δ	
M	C <sub>p</sub>	M	C <sub>p</sub>	M	C <sub>p</sub>	M	C <sub>p</sub>	M	C <sub>p</sub>	M	C <sub>p</sub>
7.54	.0227	3.74	.0945	2.47	.212	1.81	.336	1.97	.580	2.12	.810
10.50	.0205	5.21	.0849	3.44	.191	2.52	.302	2.61	.536	2.77	.765
13.90	.0188	6.90	.0795	4.55	.176	3.35	.280	3.42	.506	3.66	.729
		9.00	.0740	5.93	.166	4.37	.264	4.50	.482	4.78	.707
		11.88	.0704	7.83	.158	5.77	.251	5.87	.469	6.99	.695
		10.45	.154			7.53	.244	8.58	.460		
						11.00	.239				

TABLE XVIII

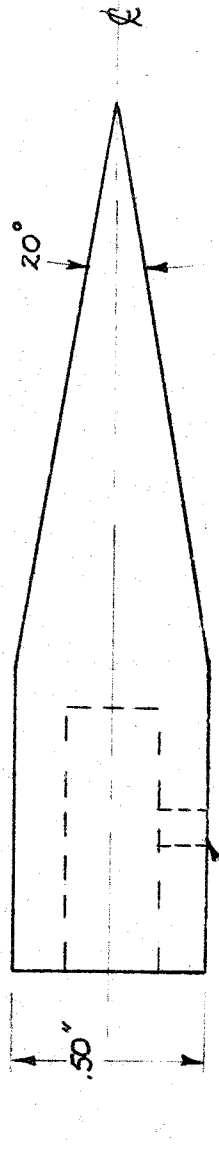
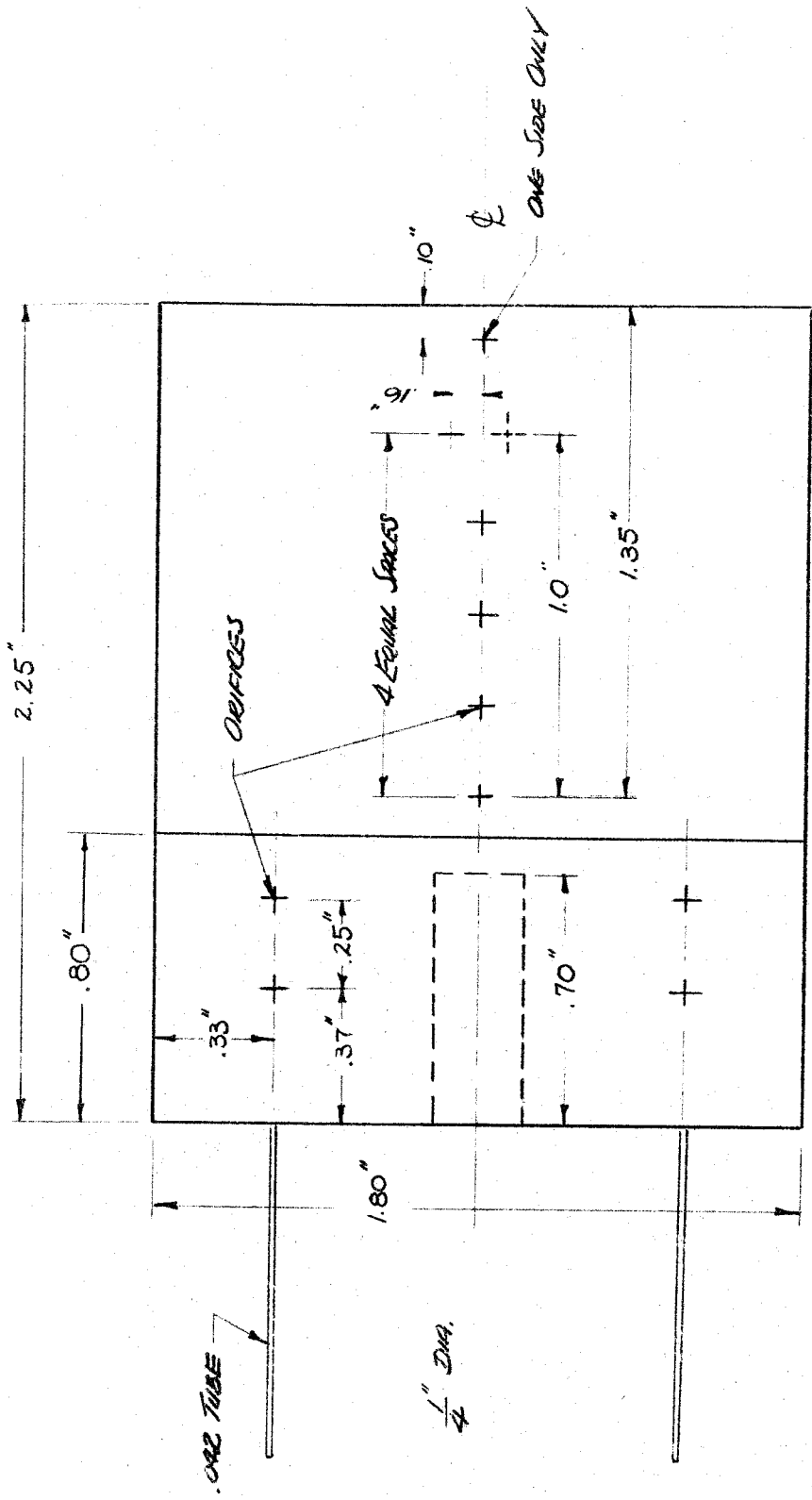
$C_L$  vs M  
Wedge,  $\delta = 20^\circ$

$\alpha = 2^\circ$

M	Oblique Shock	First Order	Second Order	Hypersonic Similitude
2.0	.1229	.0792	.1102	.0907
4.0	.0673	.0353	.0634	.0730
6.0	.0617	.0226	.0510	.0658
8.0	.0599	.0171	.0443	.0587
10.0	.0580	.0144	.0414	.0556
12.0	.0540	.0114	.0386	.0576

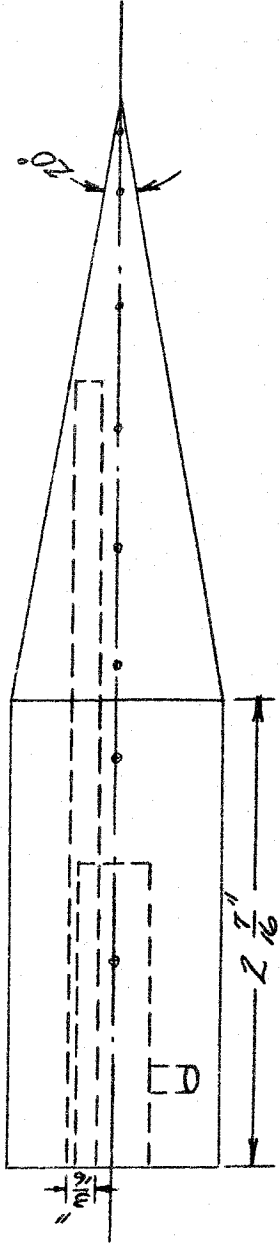
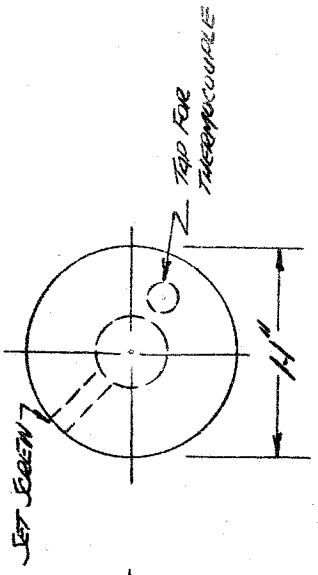
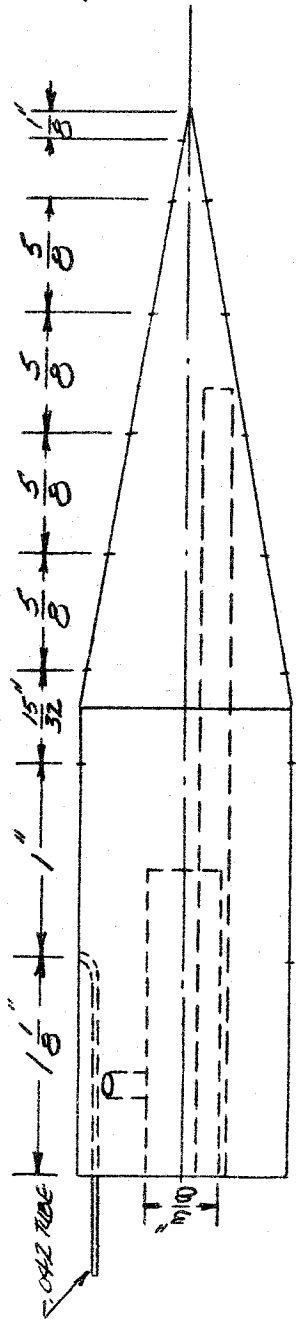
$\alpha = 4^\circ$

M	Oblique Shock	First Order	Second Order	Hypersonic Similitude
2.0	.2391	.1590	.2197	.2221
4.0	.1418	.0714	.1263	.1457
6.0	.1268	.0457	.1006	.1307
8.0	.1211	.0352	.0892	.1300
10.0	.1154	.0276	.0836	.1331
12.0	.1154	.0228	.0778	.1282



SET SCREW

PART NO.	NAME	NO. REQ.	MATERIAL DESC.	MATERIAL SPEC.	WEIGHT
<b>CALIFORNIA INSTITUTE OF TECHNOLOGY</b>					
<i>FIG 1 WEDGE</i>					
<i>HYPERSONIC MODEL</i>					
DRAWN BY			MATERIAL SPEC.		
TRACED BY			CHECKED BY		
APPROVED BY			DATE		
COURSE NO.			SCALE <i>2:1</i>		
SECTION NO.			DWG. NO.		
FINISH			HEAT TREAT		
ALL DIMENSIONS IN INCHES LIMIT ON DIMENSIONS — UNLESS OTHERWISE NOTED			ANGULAR $\pm \frac{1}{2}^\circ$ FRACTIONAL $\pm \frac{1}{32}$ DECIMAL $\pm .010$		
NUMBERS ARE SURFACE ROUGHNESS IN MICROINCHES $\sqrt{16}$ ROUGH MACHINE FINISH $\sqrt{250}$ SMOOTH MACHINE FINISH $\sqrt{40}$ ROUGH GRIND			$\sqrt{16}$ FINISH GRIND $\sqrt{2}$ FINE GRIND, LAP $\sqrt{1/4}$ POLISH		



ALL DIMENSIONS IN INCHES } ANGULAR  $\pm 1/2^\circ$   
 LIMIT ON DIMENSIONS ——— } FRACTIONAL  $\pm 1/32$   
 UNLESS OTHERWISE NOTED } DECIMAL  $\pm .010$

NUMBERS ARE SURFACE ROUGHNESS IN MICROINCHES

$\sqrt{R}$  ROUGH MACHINE FINISH  $\sqrt{16}$  FINISH GRIND  
 $\sqrt{250}$  SMOOTH MACHINE FINISH  $\sqrt{2}$  FINE GRIND, LAP  
 $\sqrt{40}$  ROUGH GRIND  $\sqrt{1/4}$  POLISH

FINISH

HEAT TREAT

PART NO.	NAME	NO. QD.	MATERIAL DESC.	MATERIAL SPEC.	WEIGHT
<b>CALIFORNIA INSTITUTE OF TECHNOLOGY</b>					
DRAWN BY					
TRACED BY					
CHECKED BY					
APPROVED BY					
DATE					
COURSE NO.					
SECTION NO.					
SCALE FULL					
DWG. NO.					
NO.					

FIG 2 CONE  
 HYPERSONIC MODEL

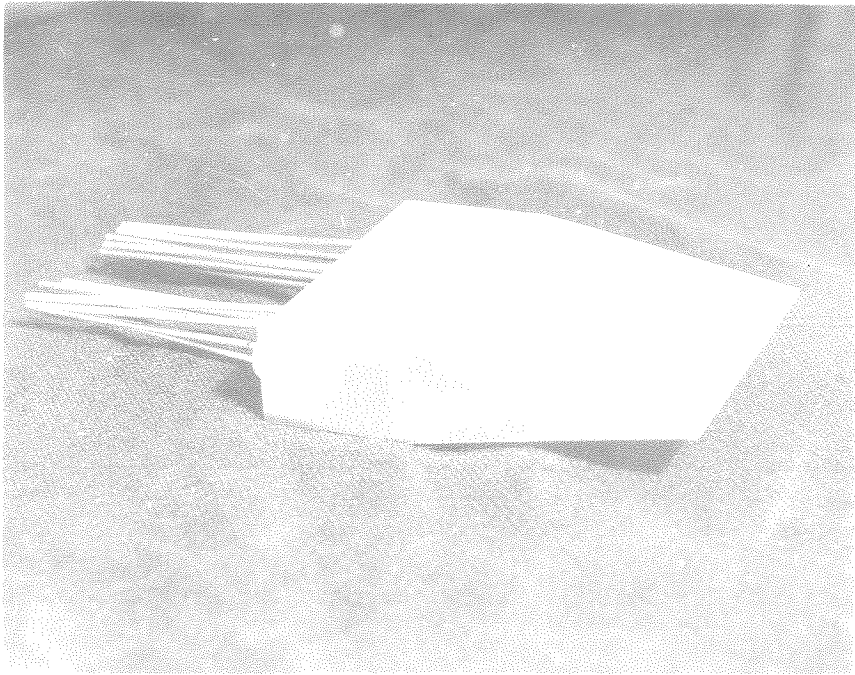


Fig. 3 - 20° WEDGE

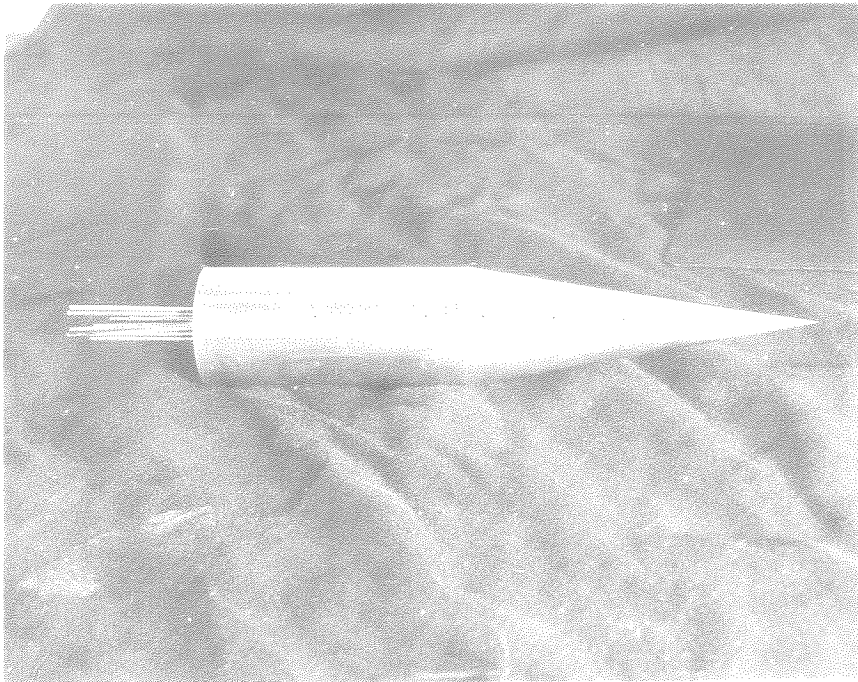
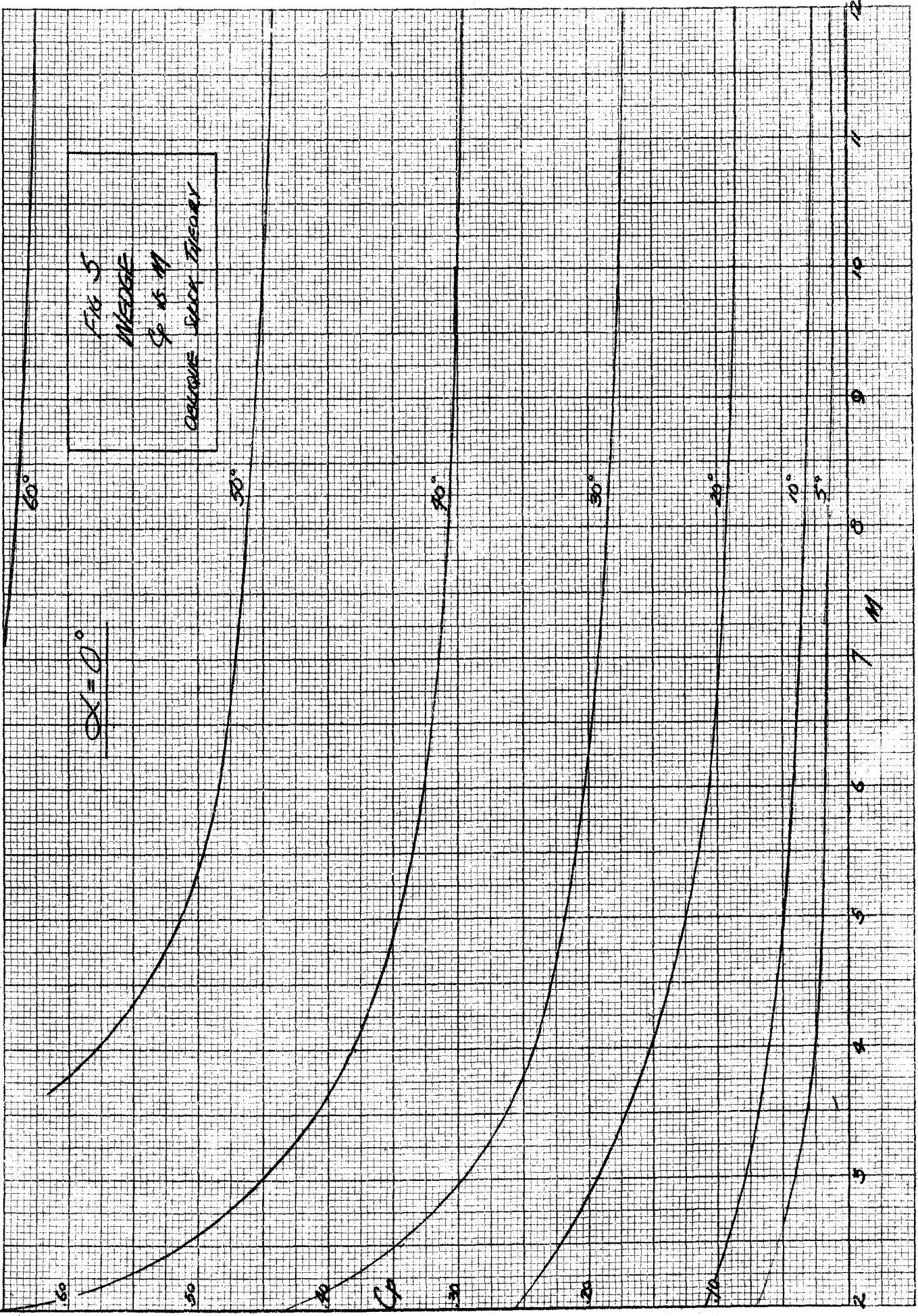


Fig. 4 - 20° CONE

FIG 5  
 WEDGE  
 $\phi = 15^\circ$   
 COLLAPSE STACK THEORY

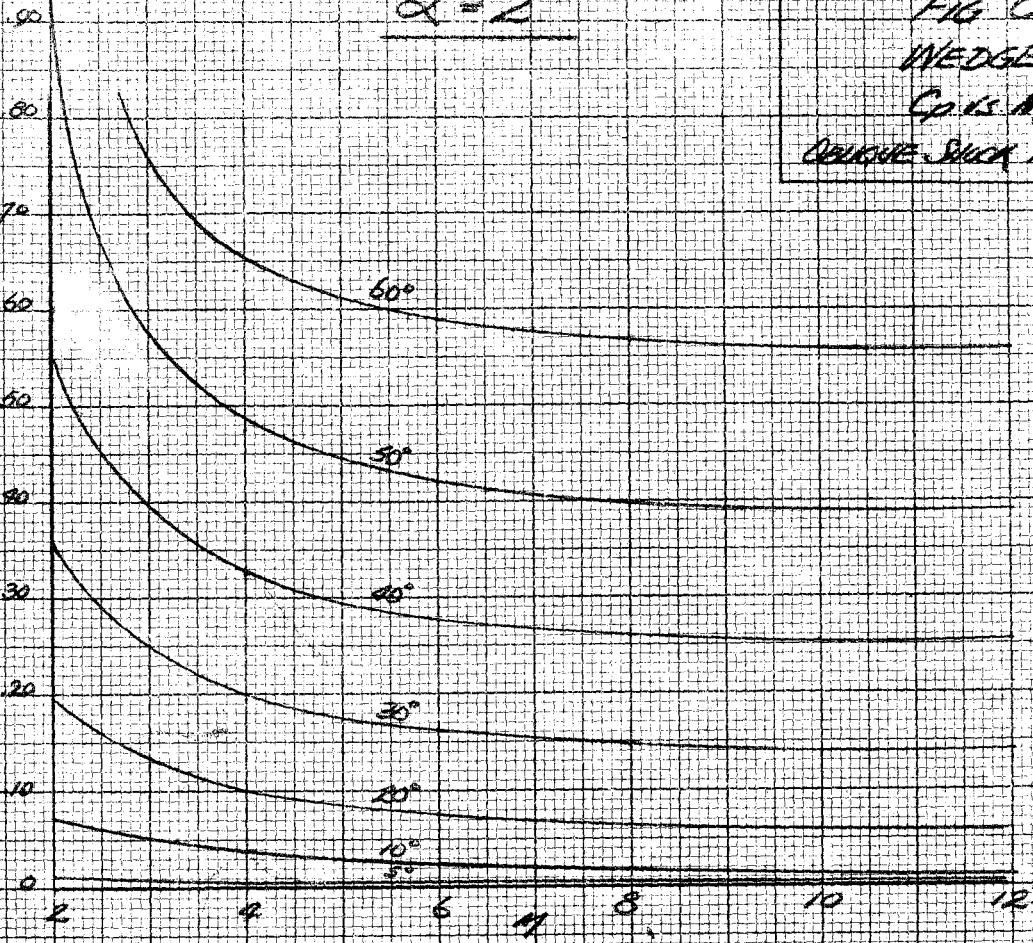
$\alpha = 0^\circ$



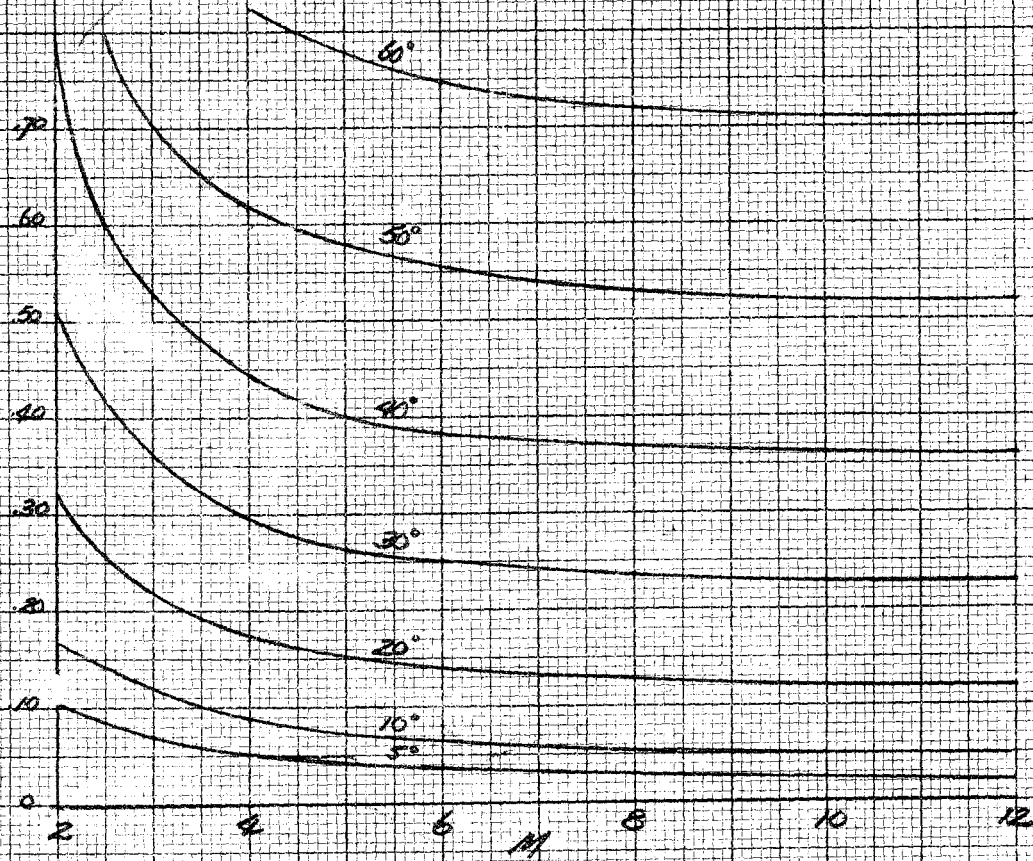
$\alpha = 2^\circ$

FIG 5  
WEDGE  
Cp 15 M  
DELTA-SLICK THEORY

C<sub>upper</sub>



C<sub>lower</sub>





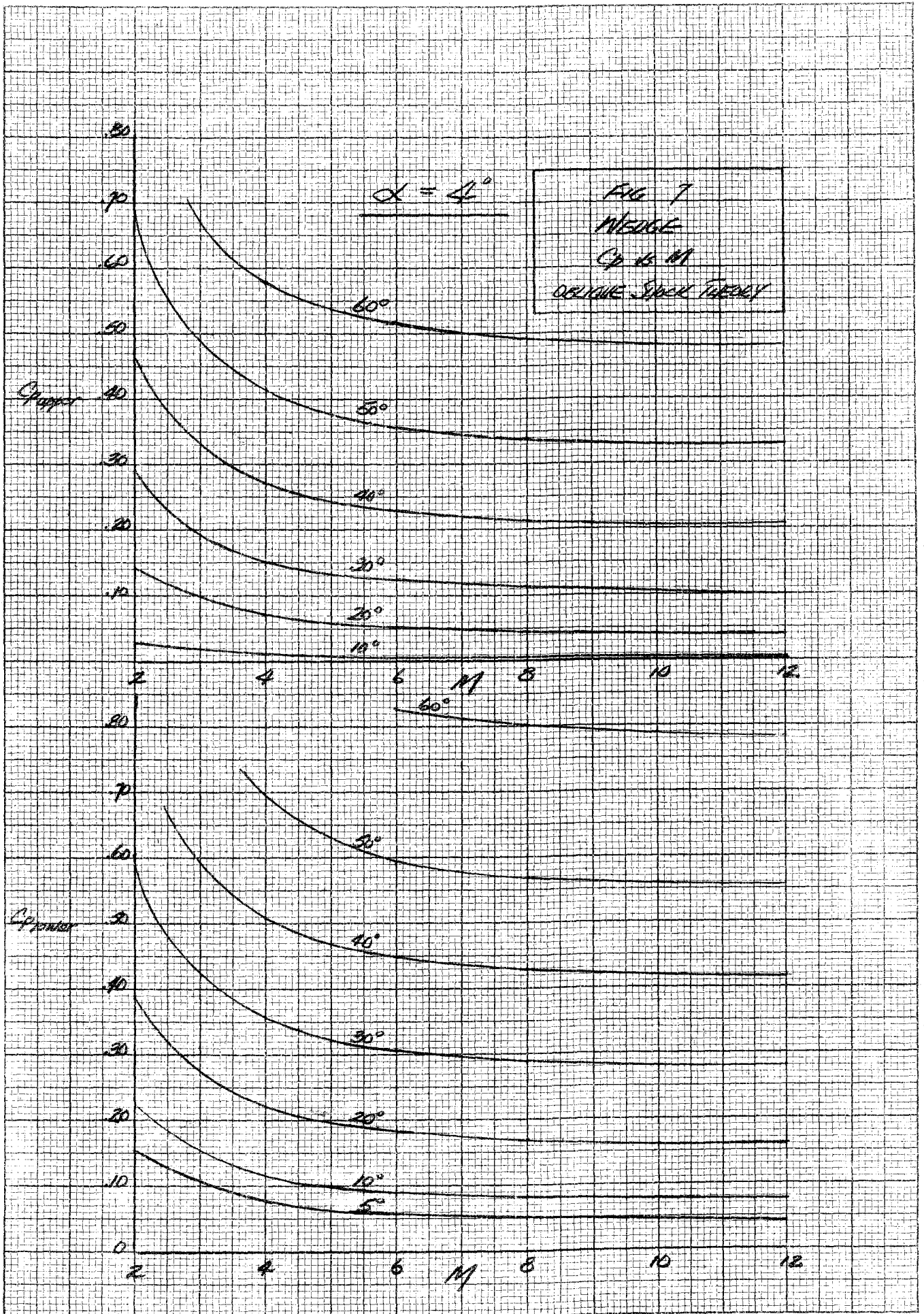




FIG 3  
 COME  
 Sp. 10.17  
 EAST THEORY

$\alpha = 0^\circ$

60°

50°

40°

30°

20°

10°

7 M

6

5

4

3

2

9

8

7

6

5

4

3

2

10

9

8

7

6

5

4

3

2

11

10

9

8

7

6

5

4

3

2

12

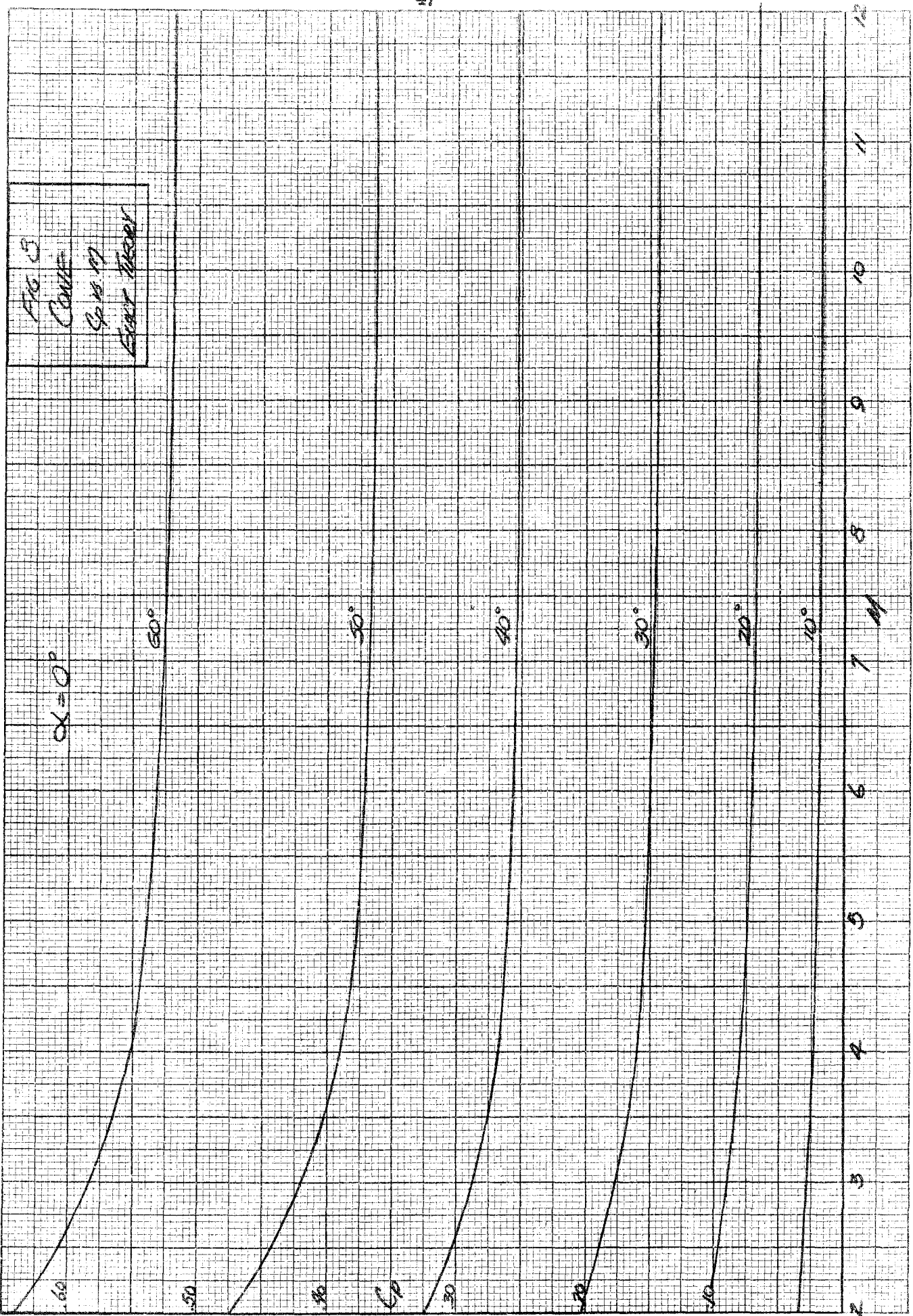
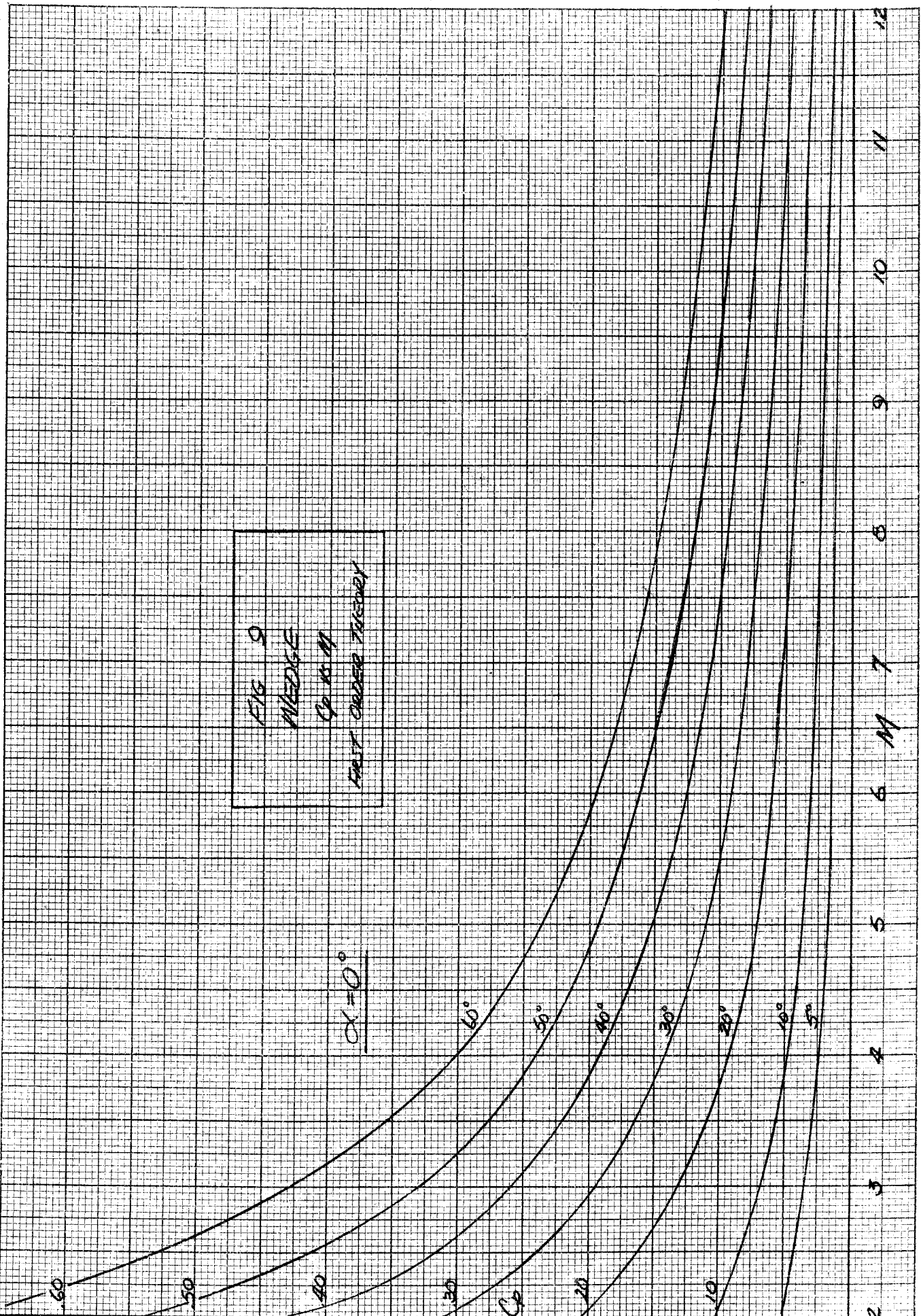
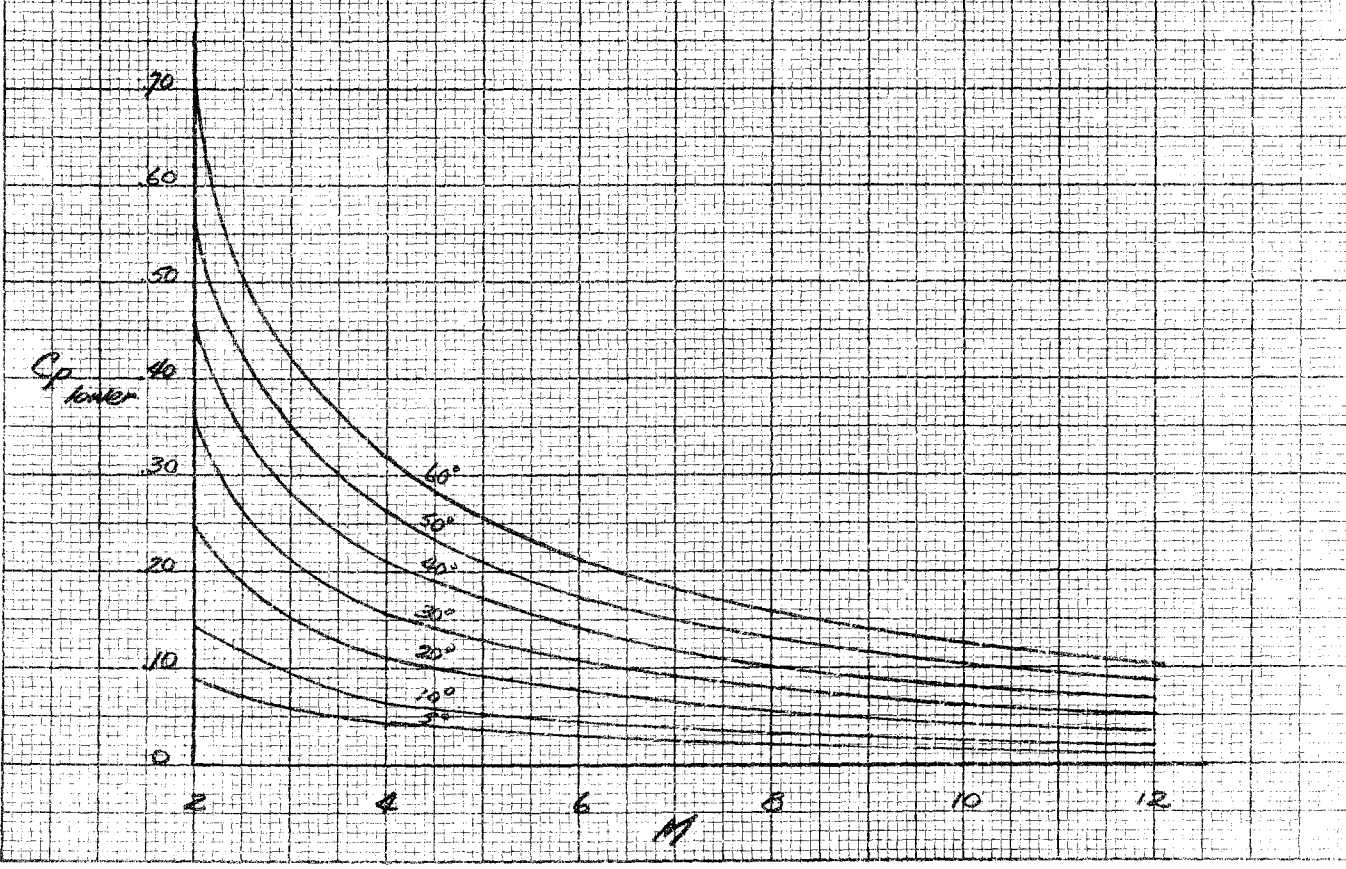
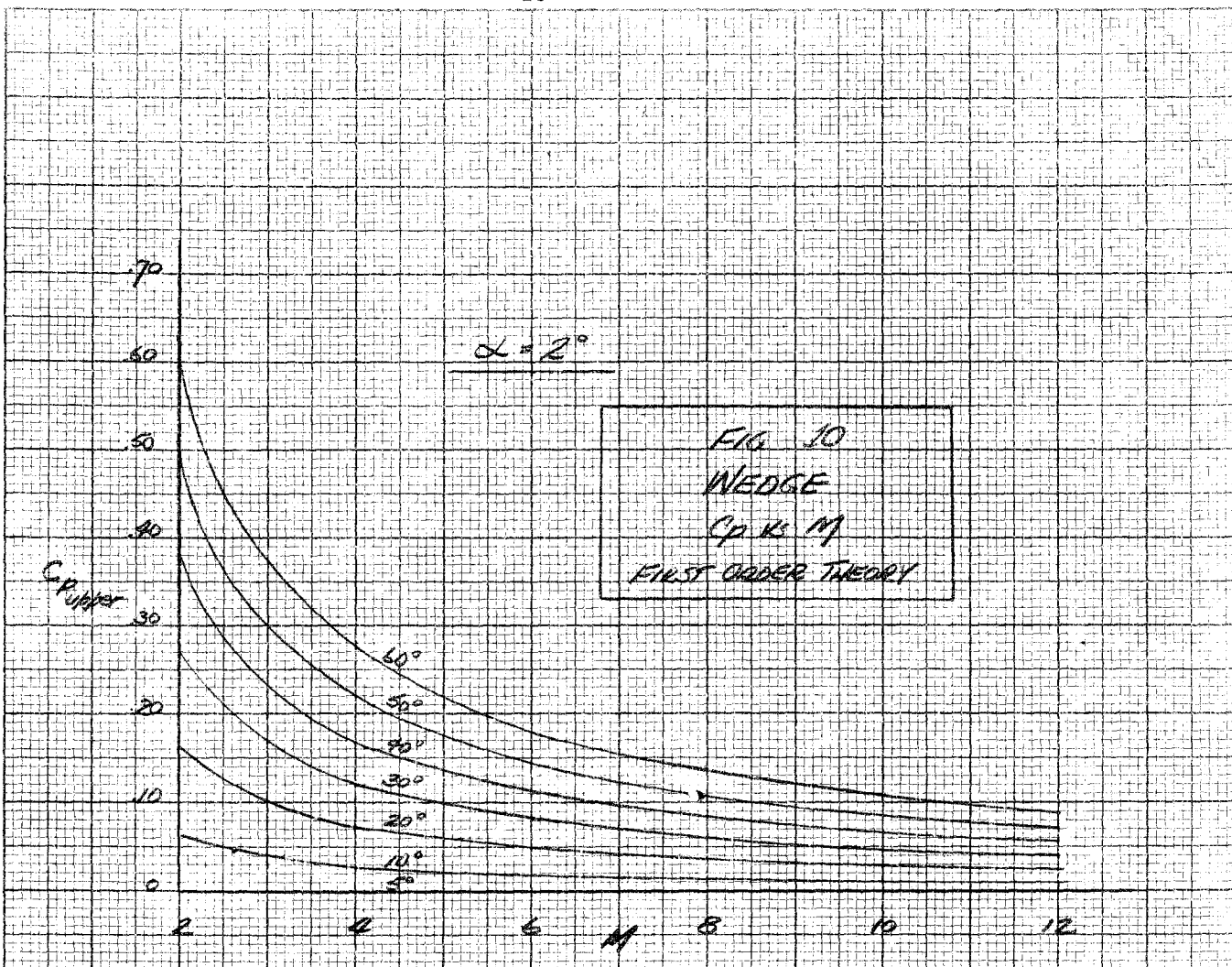


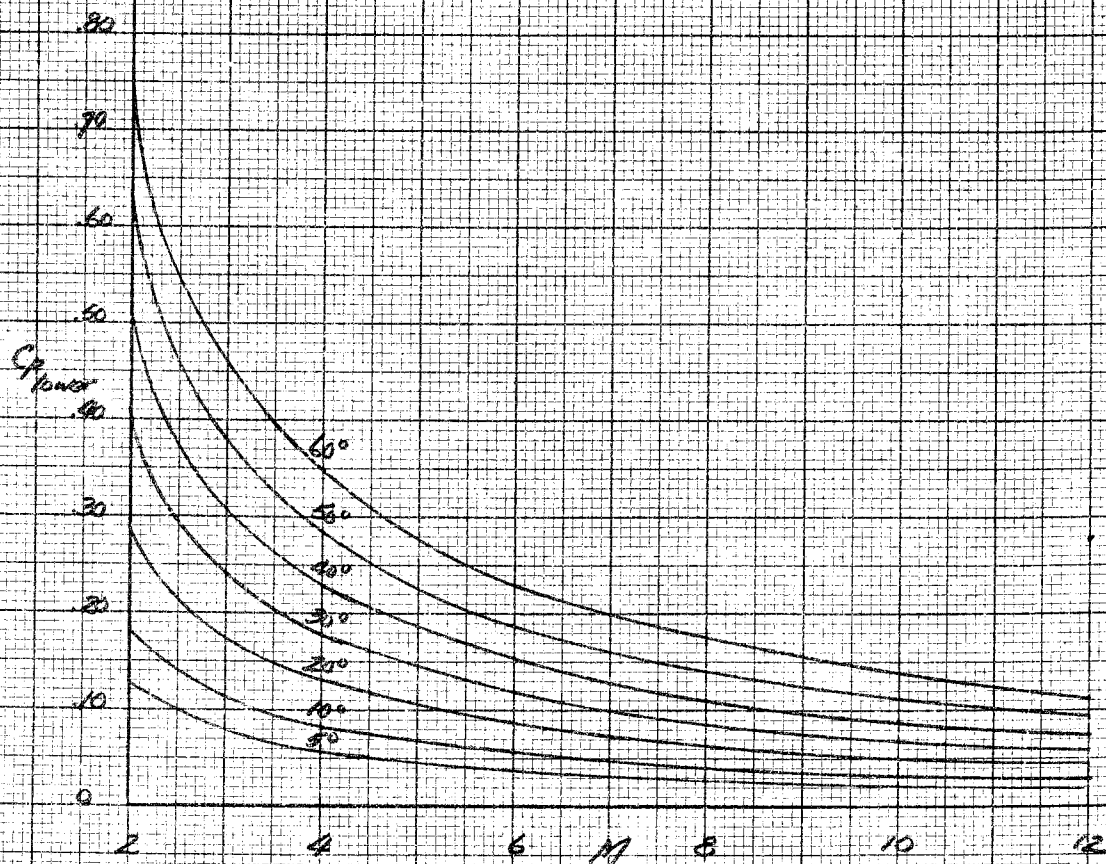
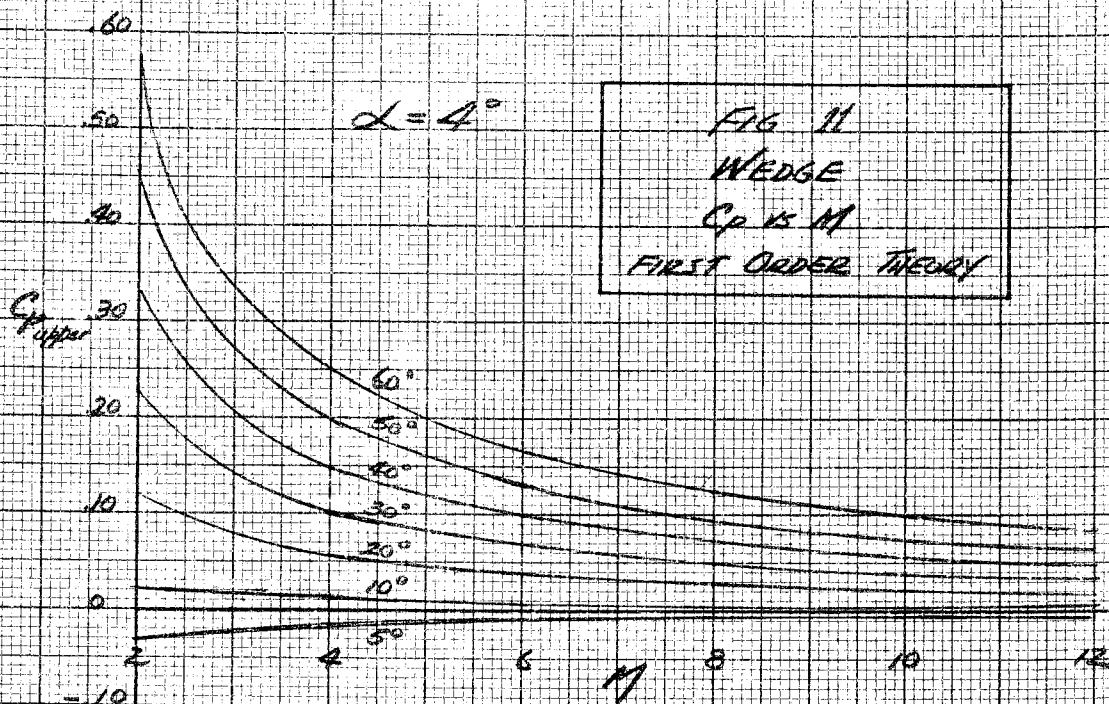
FIG 9  
WEDGE  
Gr. 15 M  
FIRST ORDER THEORY

$\alpha = 0^\circ$









512 114  
 12012  
 G. H. M.  
 FURTHER THEORY

$\alpha = 0^\circ$

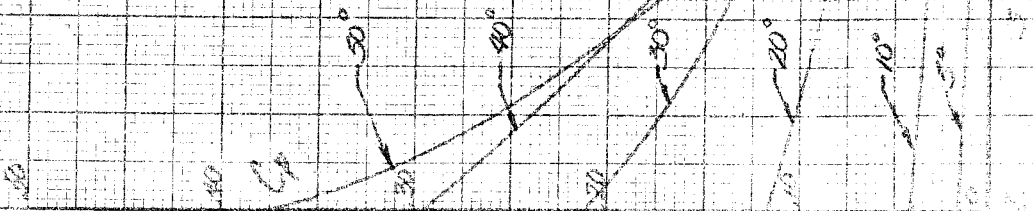
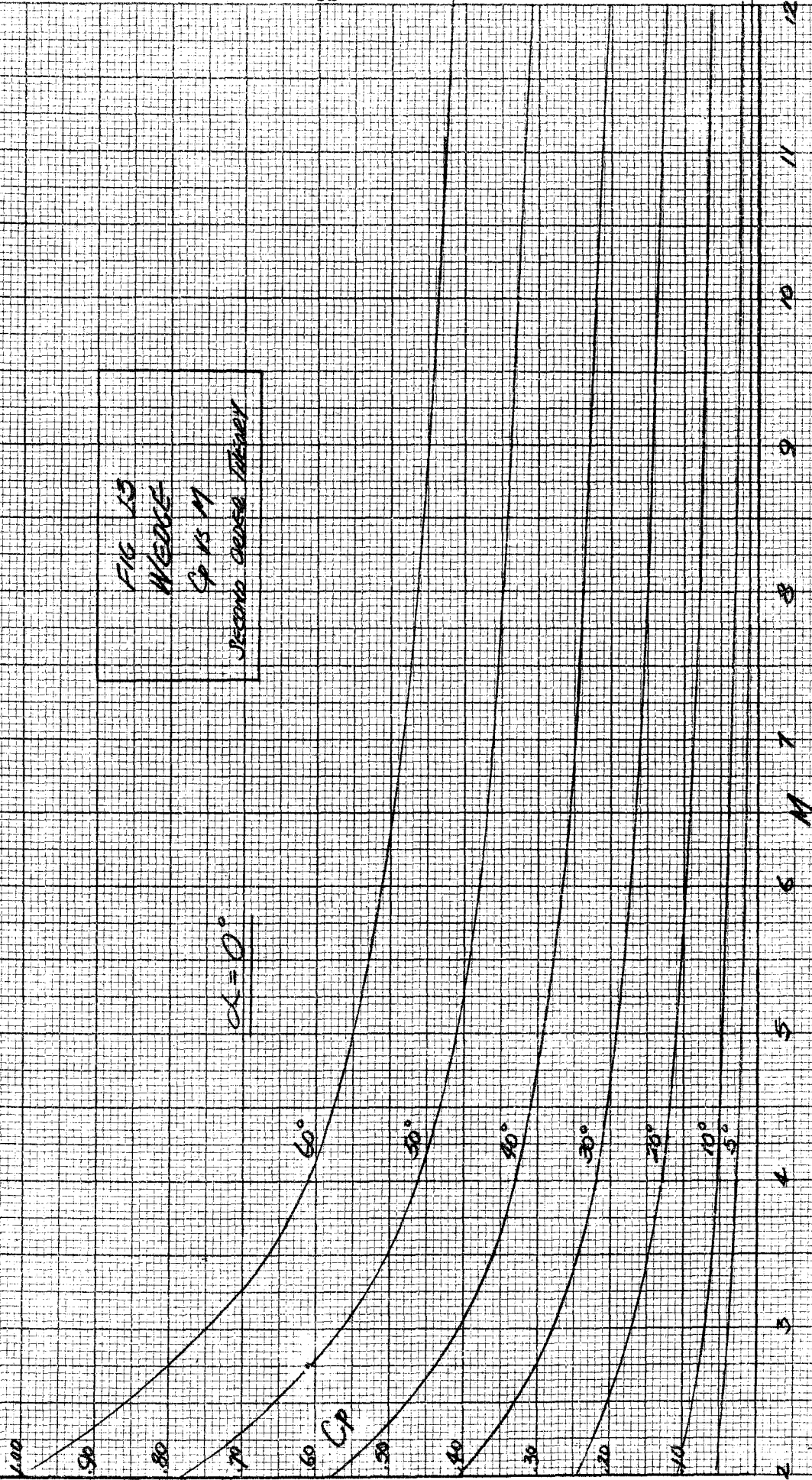


FIG 13  
 WEDGE  
 Sp 15. M  
 Second dense layer

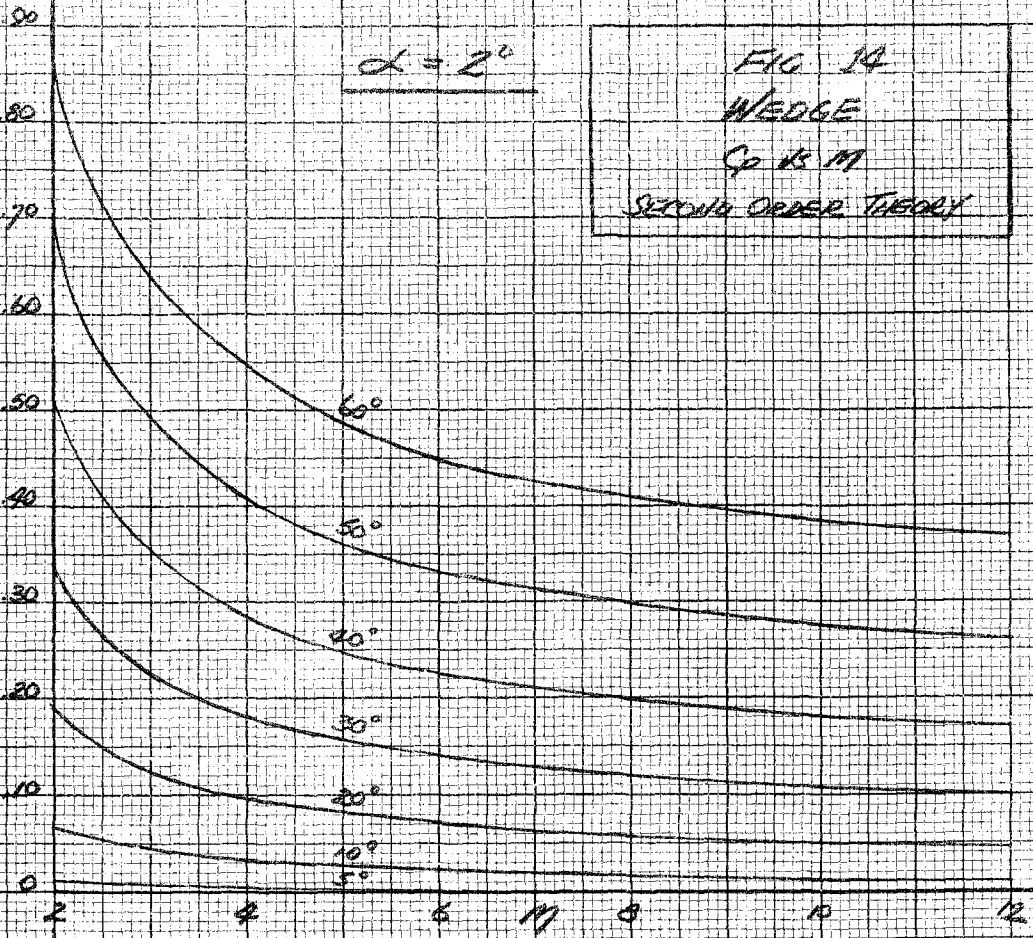
$\alpha = 0^\circ$



$\alpha = 2^\circ$

FIG. 14  
WEDGE  
Cp vs M  
SECOND ORDER THEORY

Cp<sub>upper</sub>



Cp<sub>lower</sub>

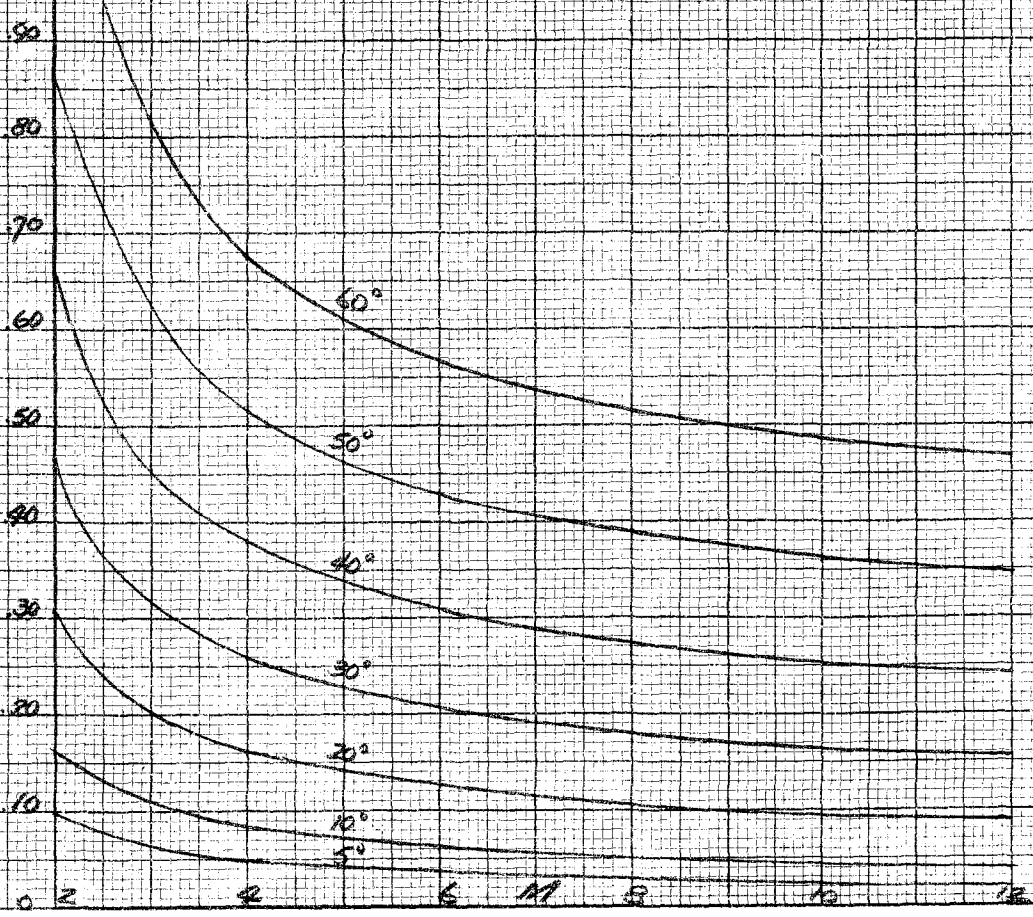








FIG 16  
 CONVE  
 Cp vs M  
 SECOND ORDER THEORY

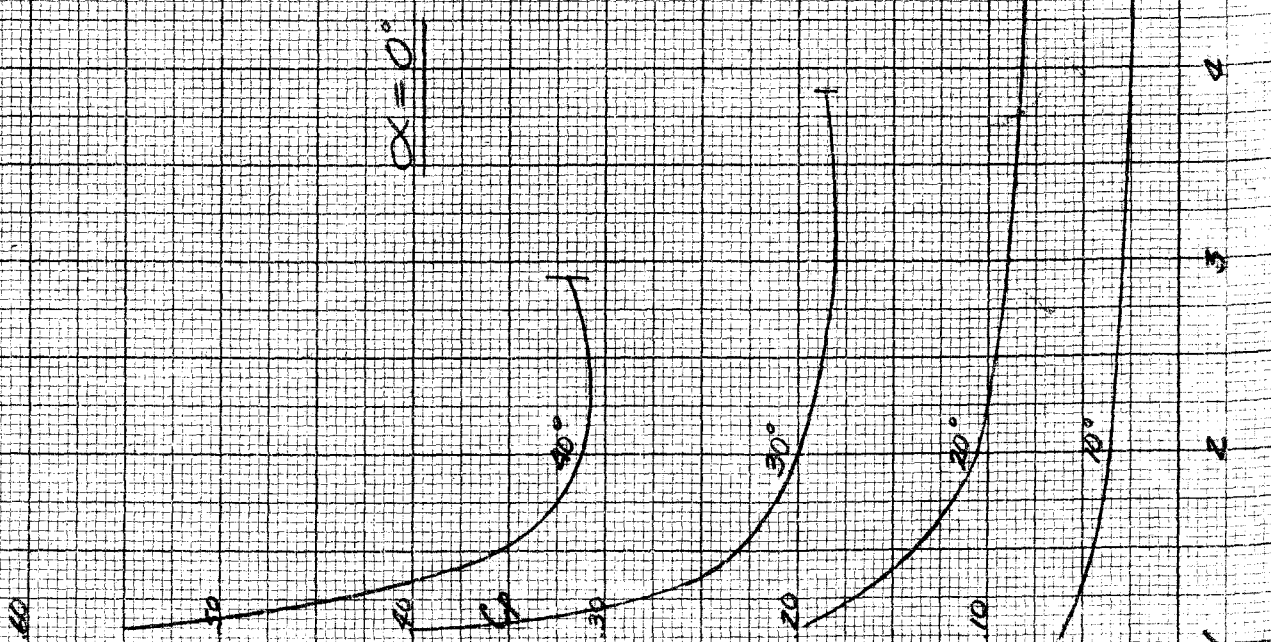


FIG. 17  
HYPERBOLIC SINGULARITY PARAMETER

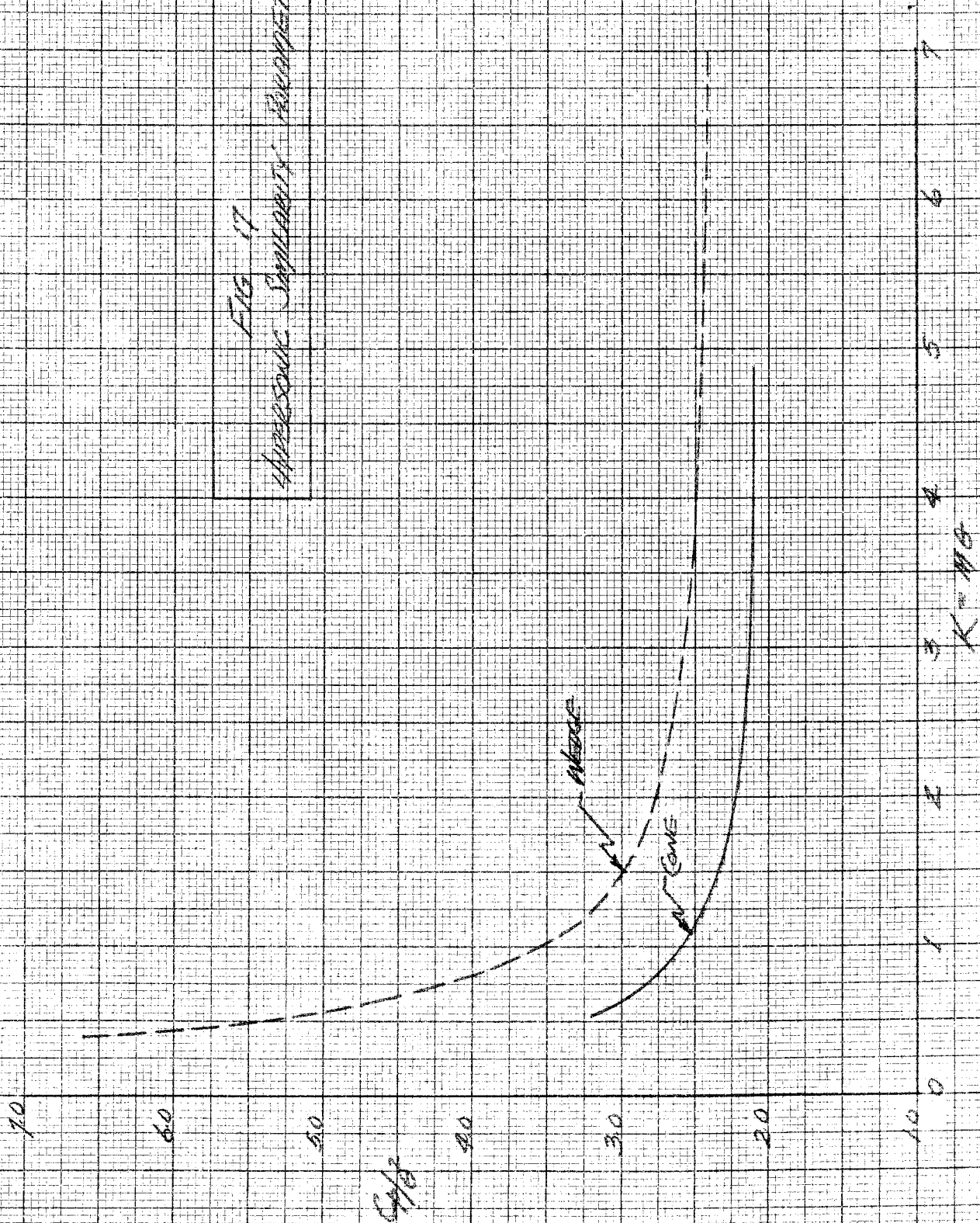
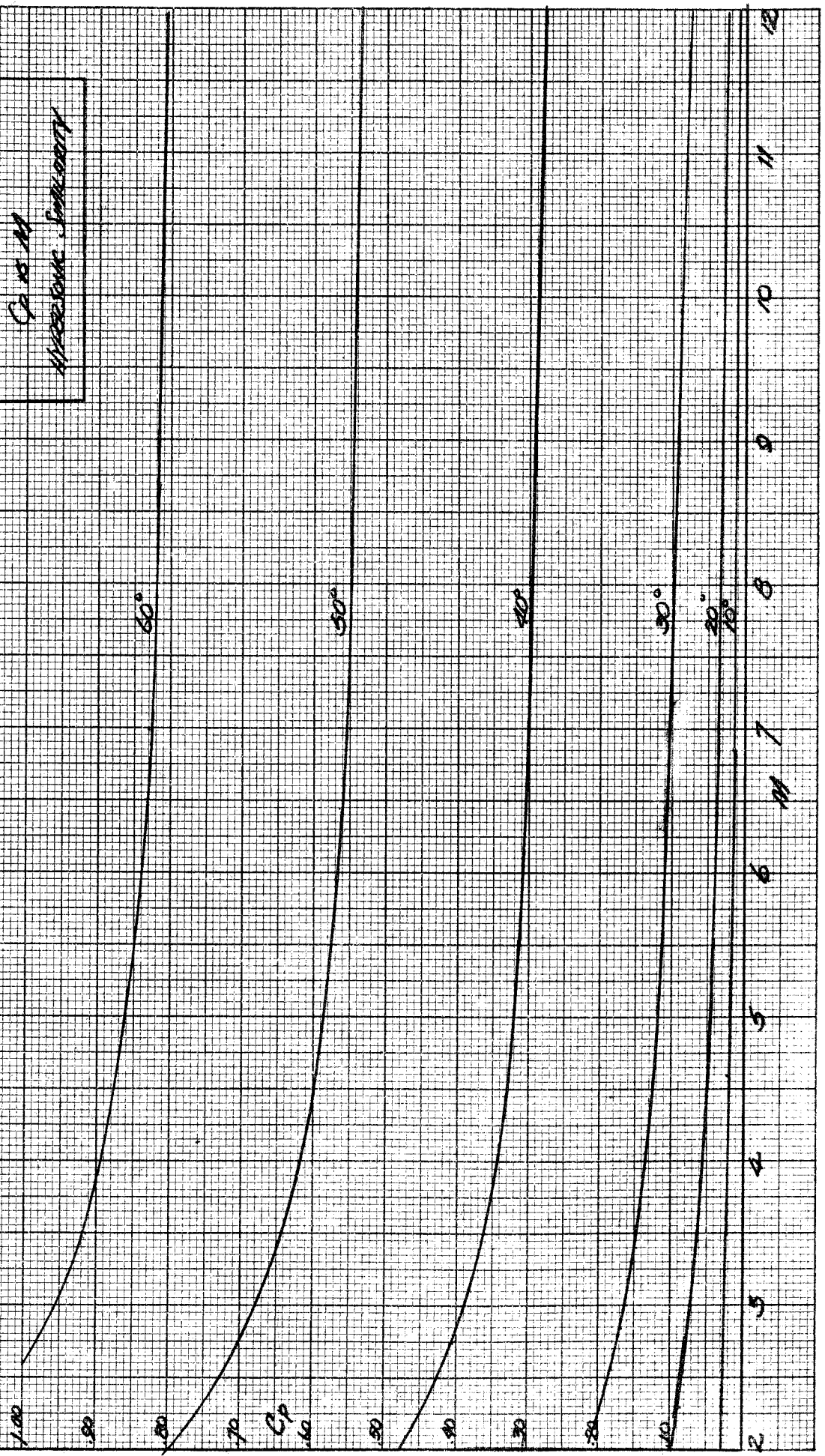


FIG 10  
 WEDGE  
 G.B.M.  
 HYPERBOLIC SIMILARITY

$\alpha = 0^\circ$



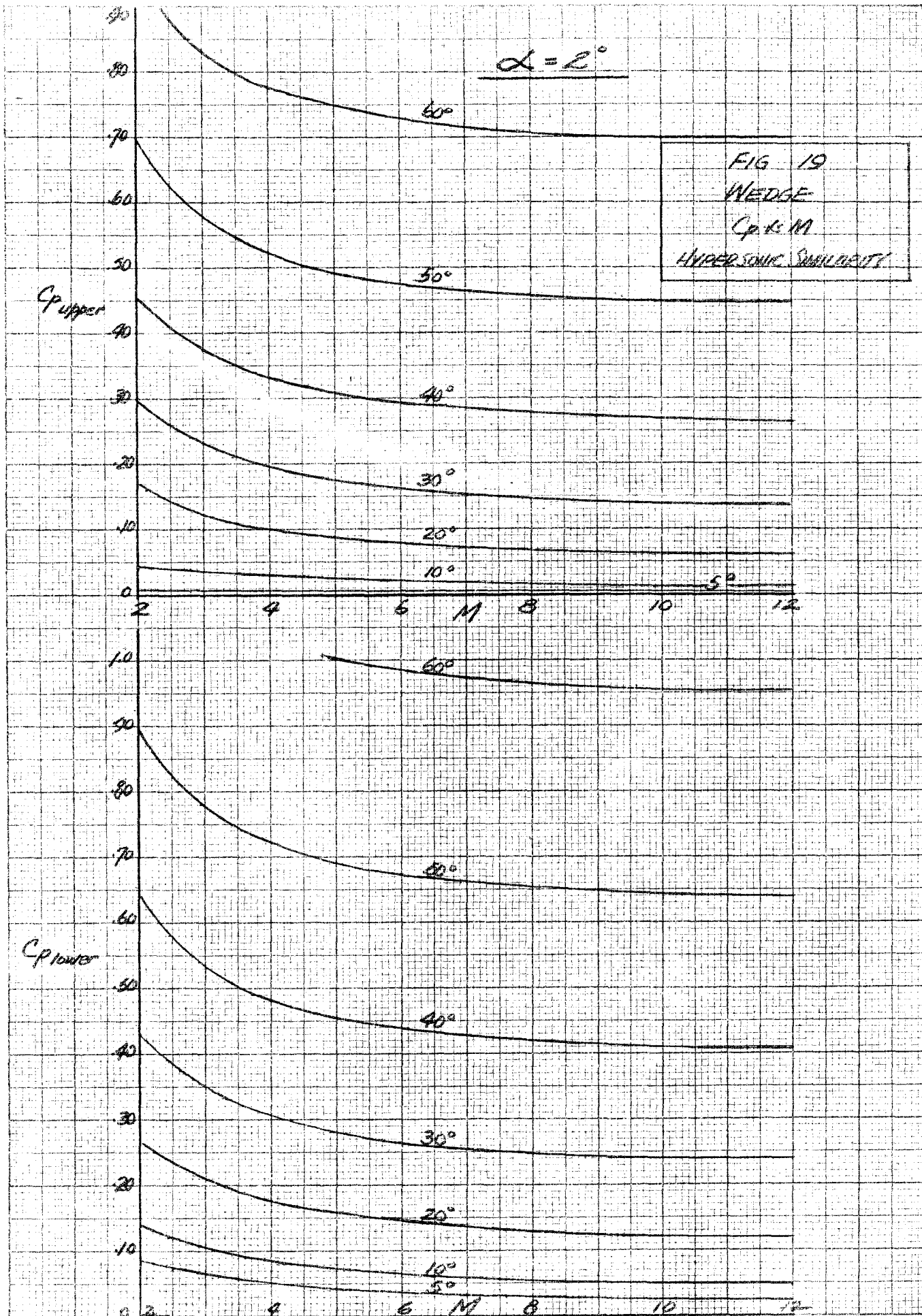




FIG 20  
WEDGE  
Cp vs M  
SUPERSONIC SIMILARITY

$\alpha = 4^\circ$

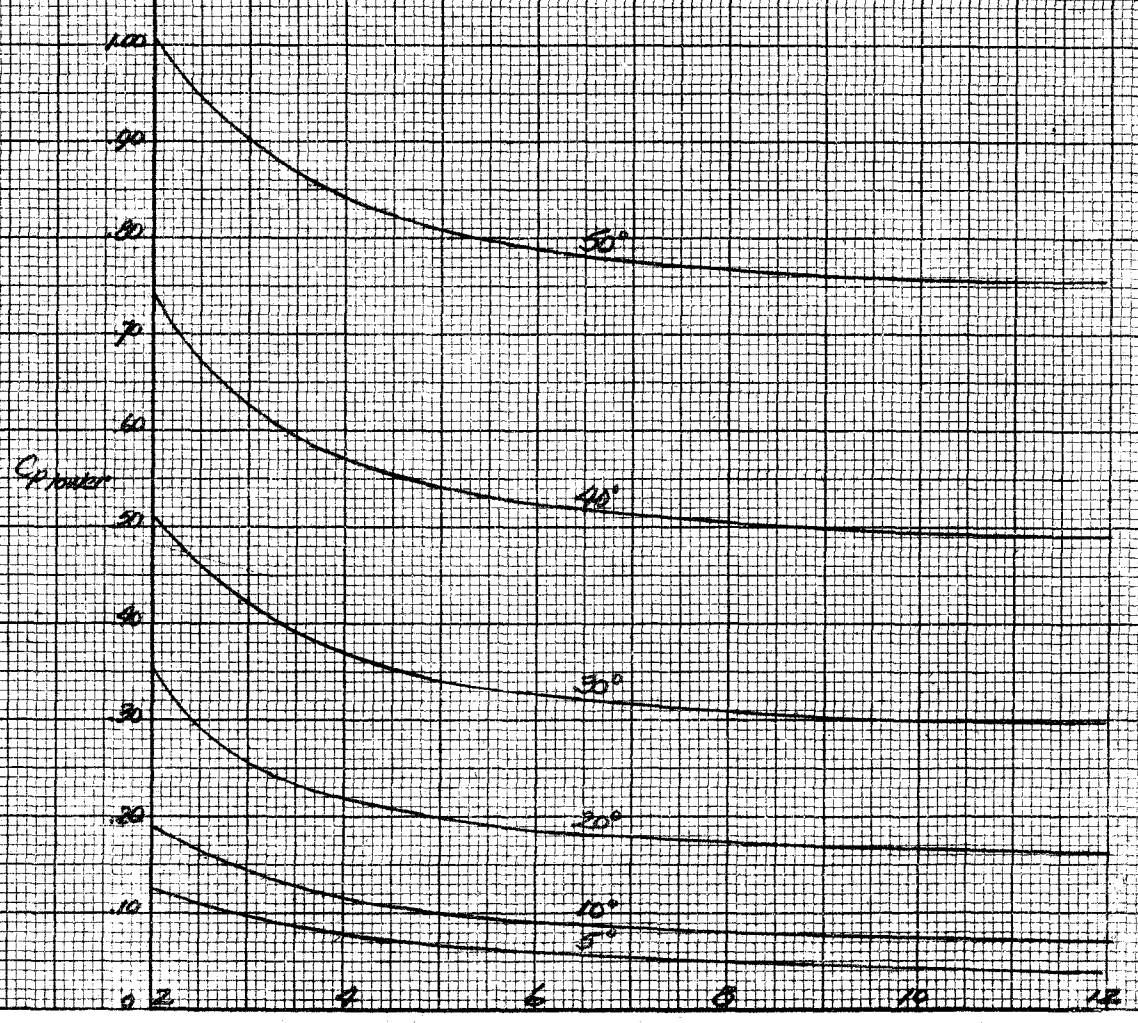
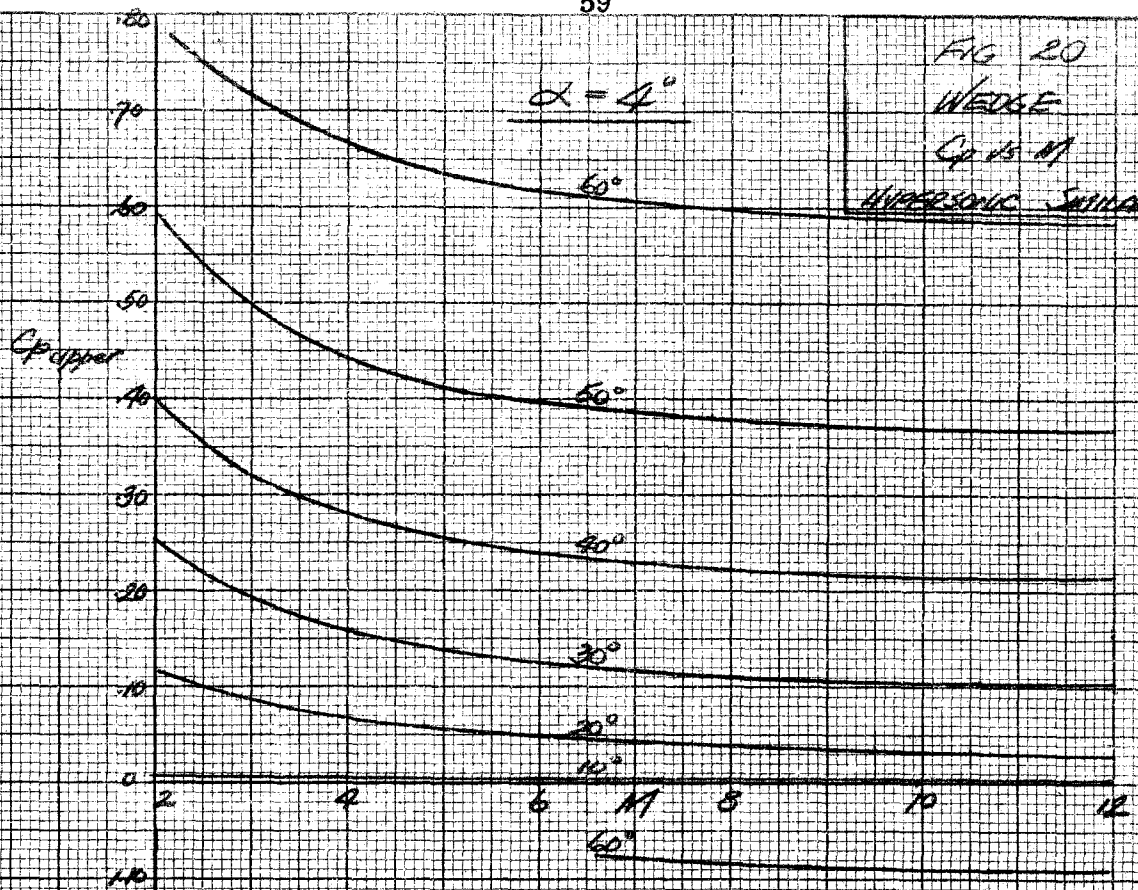


FIG 21  
 CONE  
 Cp vs M  
 ALPHASINUS SENSIBILITY

$\alpha = 0^\circ$

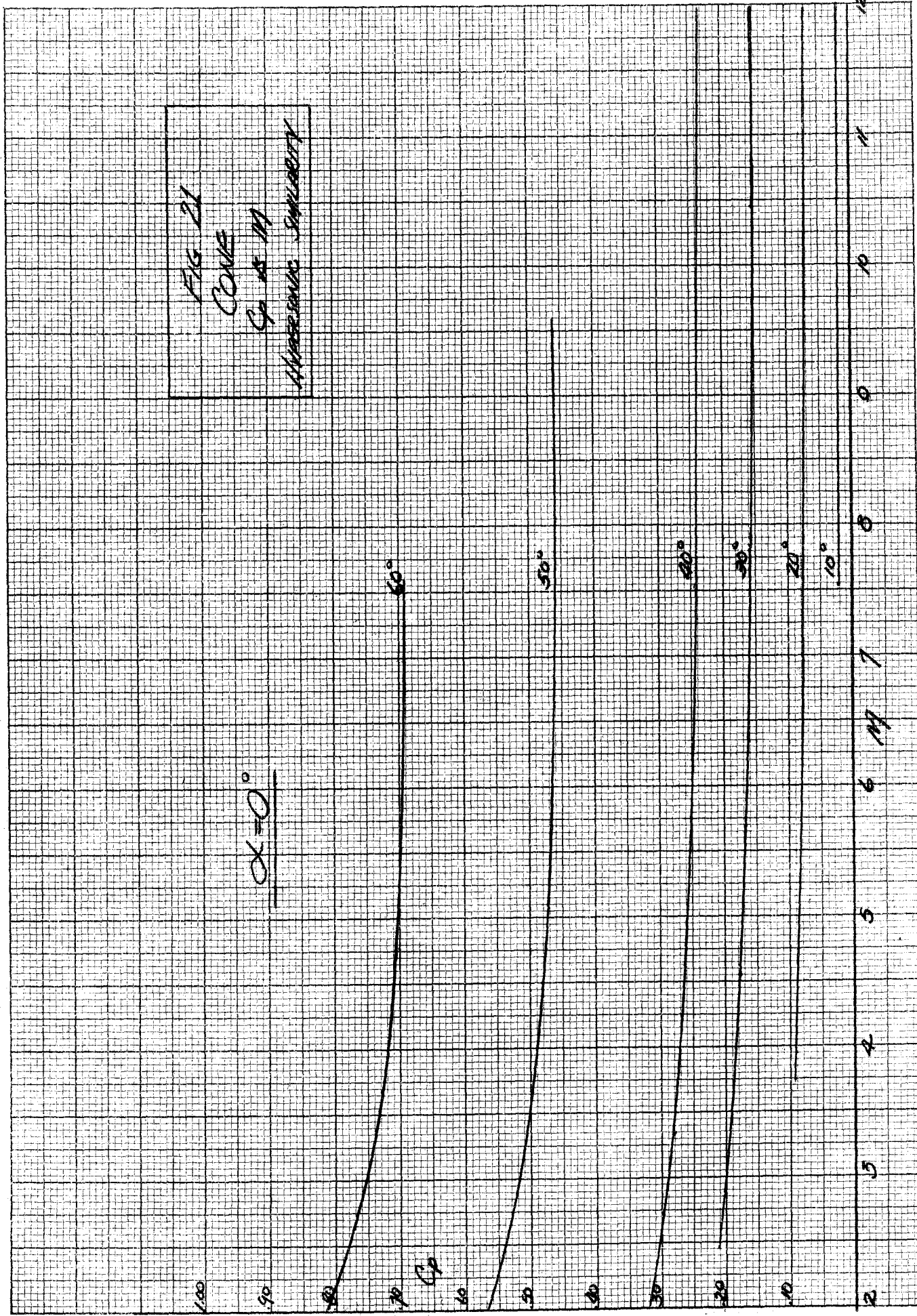


FIG 22  
 $C_p$  vs  $M$   
 VARIOUS THEORIES FOR  
 20° WEDGE AND CONE  
 $\alpha = 0^\circ$

WEDGE

OBLIQUE SHOCK

FIRST ORDER

SECOND ORDER

HYPERSONIC SIMILARITY

$C_p$

.26  
 .24  
 .22  
 .22  
 .18  
 .16  
 .14  
 .12  
 .10  
 .08  
 .06  
 .04  
 .02  
 0

2 4 6 8 10 12  
 $M$

CONE

$C_p$

.10  
 .08  
 .06  
 .04  
 .02  
 0

2 4 6 8 10 12  
 $M$

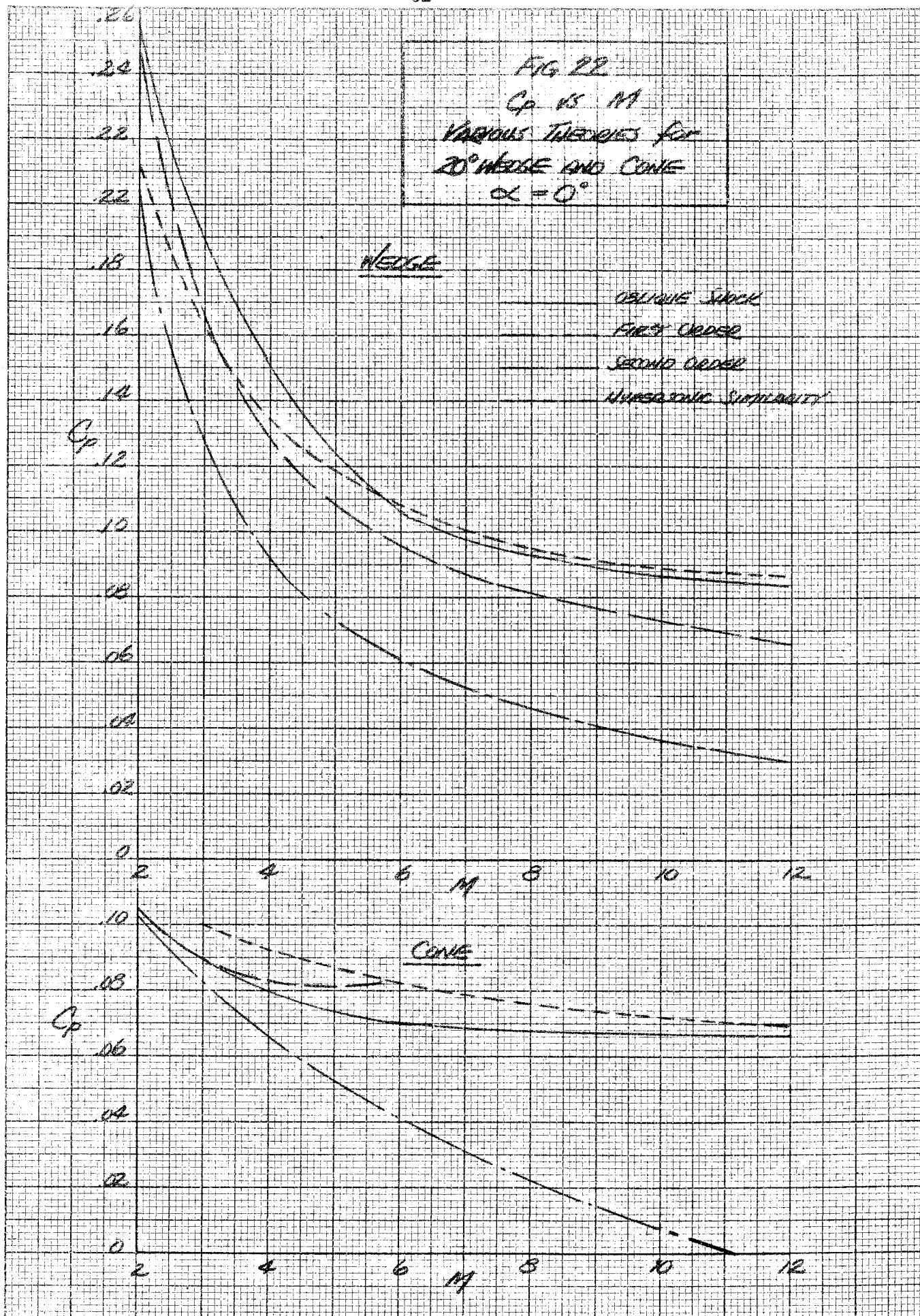




FIG 23  
 $C_L$  vs  $M$   
 20° WEDGE

